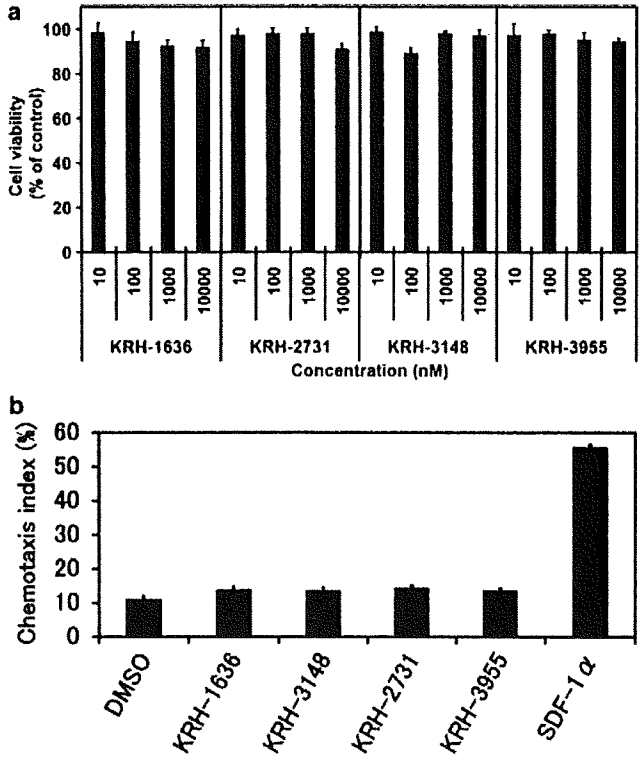

Fig. 2. CXC chemokine receptor-4 (CXCR4) antagonists exhibited neither cytotoxic nor agonistic effects. (a) Increasing amounts of CXCR4 antagonists were examined for their cytotoxic effect on E6-1 cells. (b) CXCR4 antagonists (10 μM) or stromal cell-derived factor-1α (SDF-1α) (100 ng/mL) were added to the lower wells in a chemotaxis assay and were incubated at 37°C for 3 h. The treated E6-1 cells were evaluated for the chemotaxis index. DMSO, dimethyl sulfoxide.

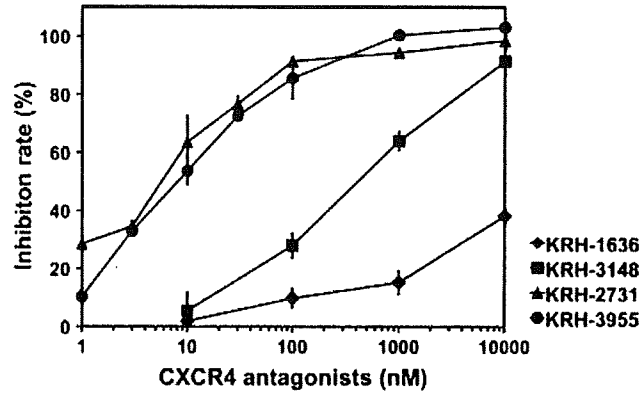

Fig. 3. Dose-dependent effect of CXC chemokine receptor-4 (CXCR4) antagonists on inhibition of stromal cell-derived factor-1α (SDF-1α)-mediated chemotaxis. E6-1 cells were pretreated with each concentration of CXCR4 antagonists at 37°C for 1 h, followed by incubation with 100 ng/mL of SDF-1α for 3 h. The cells were evaluated for the chemotaxis index. The inhibition rate was calculated as the percentage inhibition of chemotaxis by the antagonists.

Table 1. Inhibitory effects of CXCR4 antagonists on SDF-1α-mediated chemotaxis and HIV-1 infection

CXCR4 antagonists	CXCR4 (EC_{50}, nM)	
	Chemotaxis	HIV-1
KRH-1636	>10 000	42
KRH-3148	396.7	4
KRH-2731	9.2	0.9
KRH-3955	5.3	1

Next, the two cell lines were analyzed for SDF-1α-mediated chemotaxis activity; after 24 h of incubation, about 30% of both Jurkat and E6-1 migrated to the lower wells in the presence of the control medium. Since the value was the background for this chemotaxis assay, we subtracted this value from the subsequent experiments. We decided to use 400 ng/mL of SDF-1α for the chemotaxis assay as previously described by Liang *et al.*[21] It was found that SDF-1α induced a four-fold increase in the migration efficiency of E6-1 cells compared to the original Jurkat cells (Fig. 1b). Therefore, we decided to use E6-1 cells for the subsequent experiments.

Next, we attempted to optimize the experimental conditions for the SDF-1α-mediated chemotaxis assay. The chemotaxis index plateaued at approximately 60% after 3 h incubation of E6-1 cells with 400 ng/mL of SDF-1α (data not shown). We then examined the effect of increasing concentration of SDF-1α on the chemotaxis index and found that the level of chemotaxis was augmented in a dose-dependent manner and plateaued when more than 40 ng/mL of SDF-1α was used (Fig. 1c). Accordingly, the optimal condition for the chemotaxis assay in subsequent experiments was 100 ng/mL of SDF-1α for a 3h incubation period.

Next, we analyzed the cytotoxicity of CXCR4 antagonists to E6-1 cells. As indicated in Figure 2(a), the CXCR4 antagonists were not cytotoxic for E6-1 cells at a 10 μM concentration. To ascertain the possibility of these antagonists also exhibiting agonistic activities, we examined the chemotaxis activity of the antagonists. We observed that 100 ng/mL SDF-1α efficiently induced migration of E6-1; however, none of antagonists induced migration even at 10 μM (Fig. 2b). This indicated that the CXCR4 antagonists did not possess agonistic properties.

The effect of CXCR4 antagonists on the chemotaxis was investigated under the same conditions as described above. The prototype antagonist KRH-1636 inhibited the SDF-1α-mediated chemotaxis up to approximately 40% at a maximal concentration (10 μM). By contrast, KRH-3148 almost completely inhibited the chemotaxis at the maximal concentration; moreover, KRH-2731 and KRH-3955 showed the maximum inhibition rate even at 1 μM (Fig. 3). In order to quantitatively compare these efficacies, 50% effective concentration (EC_{50}) was calculated (Table 1). The results from this study clearly showed that KRH-2731 and KRH-3955 were effective at >1000-fold as compared with KRH-1636.

We further evaluated the effect of the compounds on HIV-1 infection. Anti-HIV-1 activities in nM of KRH-1636, KRH-3148, KRH-2731, and KRH-3955, which were shown as EC_{50}, were 42, 4, 0.9, and 1, respectively (Table 1). The efficacy of the antagonists was highly correlated with their inhibitory effects on HIV-1 infection by interrupting the association of the Env with CXCR4. Interestingly, inhibition of chemotaxis by KRH-1636 and KRH-3148 was relatively lower than that of HIV-1 infection compared with KRH-2731 and KRH-3955. The difference may be because action sites of KRH-2731 or KRH-3955 against CXCR4 are somewhat different from those of KRH-3148 (Sei Kumakura, unpublished data). In summary, these results demonstrate that both KRH-2731 and KRH-3955 are capable of efficiently inhibiting SDF-1α-mediated chemotaxis as well as infection of T cell–tropic HIV-1.

Discussion

The present study demonstrated that the novel CXCR4 antagonists efficiently inhibited SDF-1α-mediated chemotaxis as well as

infection of T cell-tropic HIV-1. Two compounds KRH-2731 and KRH-3955 were found to be highly potent inhibitors for both efficacies without any cytotoxicity or agonistic activity, indicating that they may be promising as anti-cancer metastasis and anti-HIV-1 drugs. In particular, both KRH-2731 and KRH-3955 efficiently inhibited calcium signaling induced by SDF-1α at a concentration of 10 nM, while KRH-3148 and KRH-1636 inhibited at 100 nM and at greater than 10 μM, respectively (Sei Kumakura *et al.*, unpublished results). This indicated that their antagonistic effects were highly correlated with their abilities to inhibit chemotaxis and HIV-1 infection.

While the Jurkat cell line expressed a smaller but almost comparable level of CXCR4 compared with E6-1 cells (Fig. 1a), their migration levels in the presence of SDF-1α were quite different (Fig. 1b). It is possible that the original Jurkat cells express non-functional CXCR4 with regard to signal transduction that is required for chemotaxis.

Tumor cells from various types of human cancers of epithelial, mesenchymal, and hematopoietic origins express high levels of CXCR4.[14,16] The interaction of SDF-1α with its receptor CXCR4 contributes to metastasis of breast cancer as well as a number of other malignancies in the lung, brain, and prostate. Furthermore, patients with cancers expressing high levels of CXCR4 have more extensive metastasis at lymph nodes compared with low CXCR4-expressing ones.[22] On this basis, the efficient CXCR4 antagonists demonstrated in this study may be highly valuable for the regulation of cancer metastasis. In fact, a synthetic peptide against CXCR4 efficiently inhibited metastasis of breast cancer in a mouse model,[21] thus providing support to our notion. However, a hurdle remains for the delivery of the peptide inihibitor to the primary focus of cancer in patients, thus impeding the clinical application of the inhibitor. In this regard, our low molecular weight CXCR4 antagonists are promising because they are non-cytotoxic and can be administered orally. In fact, KRH-3955 showed oral bioavailability of 25.6% in rats and its oral administration blocked X4 HIV-1 replication in the human peripheral blood lymphocytes and in severe combined immunodeficiency mouse system (Tsutomu Murakami *et al.*, manuscript in preparation). It is notable that AMD3100, another small non-peptide CXCR4 antagonist, has been shown to inhibit metastasis of cancer cells *in vitro* and *in vivo*.[23,24] Moreover, our preliminary data suggested that injection of the breast cancer cell line MDA-231 produced a huge tumor at the inoculated site as well as aggressive metastasis in the lungs of mice, and that our compounds partially inhibited both the primary tumor growth and the metastasis (data not shown).

In conclusion, CXCR4 antagonists, which can be orally administered, are promising agents for SDF-1α-mediated metastasis of cancer cells and also for the treatment and prophylaxis of a number of diseases related to the interaction between CXCR4 and SDF-1α, the best example of which would be an anti-HIV-1 drug.

Acknowledgments

We thank M. Kannagi and S. Yamaoka, Tokyo Medical and Dental University, for critical discussions. This work was supported by grants from the Ministry of Education, Culture, Sports, Science and Technology; the Ministry of Health, Labor and Welfare; and Human Health Science of Japan.

References

1 Ward SG, Westwick J. Chemokines: understanding their role in T-lymphocyte biology. *Biochem J* 1998; **333**: 457–70.
2 Le Y, Zhou Y, Iribarren P *et al.* Chemokines and chemokine receptors: their manifold roles in homeostasis and disease. *Cell Mol Immunol* 2004; **1**: 95–104.
3 Burger JA, Kipps TJ. CXCR4: a key receptor in the cross-talk between tumor cells and their microenvironment. *Blood* 2006; **107**: 1761–7.
4 Horuk R. Chemokine receptors. *Cytokine Growth Factor Rev* 2001; **12**: 313–15.
5 Nagasawa T, Hirota S, Tachibana K *et al.* Defects of B-cell lymphopoiesis and bone-marrow myelopoiesis in mice lacking the CXC chemokine PBSF/SDF-1. *Nature* 1996; **382**: 635–8.
6 Tachibana K, Hirota S, Iizasa H *et al.* The chemokine receptor CXCR4 is essential for vascularization of the gastrointestinal tract. *Nature* 1998; **393**: 591–4.
7 Zou YR, Kottmann AH, Kuroda M *et al.* Function of the chemokine receptor CXCR4 in haematopoiesis and in cerebellar development. *Nature* 1998; **393**: 595–9.
8 Burns JM, Summers BC, Wang Y *et al.* A novel chemokine receptor for SDF-1 and I-TAC involved in cell survival, cell adhesion, and tumor development. *J Exp Med* 2006; **203**: 2201–13.
9 Berger EA, Murphy PM, Farber JM. Chemokine receptors as HIV-1 coreceptors: roles in viral entry, tropism, and disease. *Annu Rev Immunol* 1999; **17**: 657–700.
10 Su L, Kaneshima H, Bonyhadi M *et al.* HIV-1-induced thymocyte depletion is associated with indirect cytopathogenicity and infection of progenitor cells in vivo. *Immunity* 1995; **2**: 25–36.
11 Bleul CC, Farzan M, Choe H *et al.* The lymphocyte chemoattractant SDF-1 is a ligand for LESTR/fusin and blocks HIV-1 entry. *Nature* 1996; **382**: 829–33.
12 Alkhatib G, Combadiere C, Broder CC *et al.* CC CKR5: a RANTES, MIP-1 alpha, MIP-1bata receptor as a fusion cofactor for macrophage-tropic HIV-1. *Science* 1996; **272**: 1955–8.
13 Cocchi F, DeVico AL, Garzino-Demo A *et al.* Identification of RANTES, MIP-1 alpha, and MIP-1 beta as the major HIV-suppressive factors produced by CD8+ T cells. *Science* 1995; **270**: 1811–15.
14 Balkwill F. Cancer and the chemokine network. *Nature Rev Cancer* 2004; **4**: 540–50.
15 Luker KE, Luker GD. Functions of CXCL12 and CXCR4 in breast cancer. *Cancer Lett* 2006; **238**: 30–41.
16 Muller A, Homey B, Soto H *et al.* Involvement of chemokine receptors in breast cancer metastasis. *Nature* 2001; **410**: 50–6.
17 Liotta LA. An attractive force in metastasis. *Nature* 2001; **410**: 24–5.
18 Santiago B, Baleux F, Palao G *et al.* CXCL12 is displayed by rheumatoid endothelial cells through its base amino-terminal motif on heparan sulfate proteoglycans. *Arthritis Res Ther* 2006; **8**: R43.
19 Ichiyama K, Yokoyama-Kumakura S, Tanaka Y *et al.* A duodenally absorbable CXC chemokine receptor 4 antagonist, KRH-1636, exhibits a potent and selective anti-HIV-1 activity. *Proc Natl Acad Sci USA* 2003; **100**: 4185–90.
20 Tamamura H, Hori A, Kanzaki N *et al.* T140 analogs as CXCR4 antagonists identified as anti-metastatic agents in the treatment of breast cancer. *FEBS Lett* 2003; **550**: 79–83.
21 Liang Z, Wu T, Lou H *et al.* Inhibition of breast cancer metastasis by selective synthetic polypeptide against CXCR4. *Cancer Res* 2004; **64**: 4302–8.
22 Dewan MZ, Ahmed S, Iwasaki Y *et al.* Stromal cell-derived factor-1 and CXCR4 receptor interaction in tumor growth and metastasis of breast cancer. *Biomed Pharmacother* 2006; **60**: 273–6.
23 Yoon Y, Liang Z, Zhang X *et al.* CXC chemokine receptor-4 antagonist blocks both growth of primary tumor and metastasis of head and neck cancer in xenograft mouse models. *Cancer Res* 2007; **67**: 7518–24.
24 Li JK, Yu L, Shen Y *et al.* Inhibition of CXCR4 activity with AMD3100 decreases invasion of human colorectal cancer cells *in vitro*. *World J Gastroenterol* 2008; **14**: 2308–13.

doi: 10.1111/j.1349-7006.2009.01104.x

JOURNAL OF CLINICAL MICROBIOLOGY, Feb. 2007, p. 477–487 Vol. 45, No. 2
0095-1137/07/$08.00+0 doi:10.1128/JCM.01708-06

Use of New T-Cell-Based Cell Lines Expressing Two Luciferase Reporters for Accurately Evaluating Susceptibility to Anti-Human Immunodeficiency Virus Type 1 Drugs▽

Tomoko Chiba-Mizutani,[1,2] Hideka Miura,[1] Masakazu Matsuda,[1] Zene Matsuda,[1] Yoshiyuki Yokomaku,[1] Kosuke Miyauchi,[1] Masako Nishizawa,[1] Naoki Yamamoto,[1,2] and Wataru Sugiura[1]*

AIDS Research Center, National Institute of Infectious Diseases, Tokyo, Japan,[1] and Department of Molecular Virology and Microbiology, Tokyo Medical and Dental University, Tokyo, Japan[2]

Received 17 August 2006/Returned for modification 25 October 2006/Accepted 11 December 2006

Two new T-cell-based reporter cell lines were established to measure human immunodeficiency virus type 1 (HIV-1) infectivity. One cell line naturally expresses CD4 and CXCR4, making it susceptible to X4-tropic viruses, and the other cell line, in which a CCR5 expression vector was introduced, is susceptible to both X4- and R5-tropic viruses. Reporter cells were constructed by transfecting the human T-cell line HPB-Ma, which demonstrates high susceptibility to HIV-1, with genomes expressing two different luciferase reporters, HIV-1 long terminal repeat-driven firefly luciferase and cytomegalovirus promoter-driven renilla luciferase. Upon HIV infection, the cells expressed firefly luciferase at levels that were highly correlated (r^2 = 0.91 to 0.98) with the production of the capsid antigen p24. The cells also constitutively expressed renilla luciferase, which was used to monitor cell numbers and viability. The reliability of the cell lines for two in vitro applications, drug resistance phenotyping and drug screening, was confirmed. As HIV-1 efficiently replicated in these cells, they could be used for multiple-round replication assays as an alternative method to a single-cycle replication protocol. Coefficients of variation for drug susceptibility evaluated with the cell lines ranged from 17 to 41%. The new cell lines were beneficial for evaluating antiretroviral drug resistance. Firefly luciferase gave a wider dynamic range for evaluating virus infectivity, and the introduction of renilla luciferase improved assay reproducibility. The cell lines were also beneficial for screening new antiretroviral agents, as false inhibition caused by the cytotoxicity of test compounds was easily detected by monitoring renilla luciferase activity.

Drug resistance assays have been accepted as standard clinical tests to guide the antiretroviral therapy of human immunodeficiency virus (HIV)-infected patients who have developed resistance to drug treatment or drug-naïve patients infected with drug-resistant virus. These tests have been shown to improve treatment outcomes by selecting the most effective drugs and by minimizing the risk of treatment failure (2, 5–7, 9, 34). Drug resistance has been determined by two approaches. One is drug resistance genotyping, in which drug resistance is evaluated by sequencing the viral genes targeted by the drug, such as the HIV-1 protease and reverse transcriptase (RT) genes. The level of drug resistance is estimated by using observed mutation patterns and interpretation algorithms (23). Several protocols have been used for drug resistance genotyping, including in-house sequencing (10, 13, 38). Although these protocols differ in some aspects, e.g., the design of primers, the length of analyses, and amplification procedures, all are based on the same technical approach, modified Sanger sequencing.

The other approach to drug resistance assays is phenotyping. In this method, the levels of drug resistance of patient-derived viral isolates are evaluated by using in vitro bioassays (17, 26). Two advantages of the phenotyping assay are its ability to directly evaluate the drug susceptibilities of patient-derived viruses and the ease of interpreting its results compared to those from genotyping. This assay is especially useful in cases with a high degree of exposure to antiretroviral drugs, therefore involving many mutations. In these cases, the evaluation of resistance levels by genotyping alone may be difficult (35). In addition, the resistance levels determined by phenotyping provide important information for updating interpretation algorithms used in genotyping.

Although peripheral blood mononuclear cells (PBMC) are the natural target of HIV type 1 (HIV-1) and hence are the best candidates for host cells in phenotyping assays, reporter cell systems are more commonly used in drug susceptibility assays (1, 12, 15, 31). Reporter systems are preferred because their susceptibility to HIV-1 is stable and their output is both rapidly measured and highly reproducible compared to that of PBMC assays. Several kinds of reporter cells have been used with different reporter proteins, such as MAGI cells with β-galactosidase (21), GHOST cells with enhanced green fluorescent protein (36), MOCHA cells with secreted alkaline phosphatase (24), and CEM.NKR-CCR5-Luc cells with luciferase (31). Although these systems use different cell lines, their basic strategies for evaluating HIV infectivity are similar (21, 36). The cell lines carry a reporter protein gene regulated by the HIV-1 long terminal repeat (LTR) promoter, inducing them to

* Corresponding author. Mailing address: AIDS Research Center, National Institute of Infectious Diseases, 4-7-1 Gakuenn, Musashimurayama, Tokyo 2080011, Japan. Phone: 81-42-561-0771. Fax: 81-42-561-7746. E-mail: wsugiura@nih.go.jp.

▽ Published ahead of print on 20 December 2006.

produce the reporter protein when they are infected with HIV-1. Which reporter system is used depends on the properties of the original cell line and the installed reporter protein.

Reporter systems using MAGI and GHOST cells have the advantages of high sensitivity and rapidity in determining infectivity. However, MAGI and GHOST cells have been established from HeLa cells (21) and human osteosarcoma cells (36), respectively, which are not naturally susceptible to HIV-1. Therefore, these cells cannot propagate viruses efficiently. On the other hand, MOCHA and CEM.NKR-CCR5-Luc cell lines were established from T-cell lines and secreted alkaline phosphatase and luciferase, respectively, were installed as reporters. These reporter systems allow for the evaluation of HIV-1 infectivity by using enzymatic reactions and demonstrate greater reproducibility with wider dynamic ranges of reporter proteins. However, for these cells to produce sufficient reporter protein for accurate determinations, they must be cultured for 5 to 7 days, longer than MAGI and GHOST cells. Longer culture periods allow reporter cells to divide, which may affect the accuracy of the quantification.

Given the advantages and limitations of previously constructed reporter cell lines, we designed and tested two new reporter cell lines with dual chemokine receptors for use in drug resistance phenotypic assays and other HIV infectivity assays. The cell lines we designed have unique characteristics in that they originate from the human T-cell line HPB-Ma (16, 29, 40) and were engineered to express the CCR5 receptor and two different marker proteins, firefly luciferase (FL) and renilla luciferase (RL). FL, which is under HIV-1 LTR promoter regulation, is produced upon HIV-1 infection. Therefore, firefly luciferase activity can be used as a marker for virus infectivity. RL, which is under cytomegalovirus (CMV) promoter control, is constitutively expressed in the cells. Therefore, renilla luciferase activity can be used as a marker for cell number and viability.

MATERIALS AND METHODS

Construction of luciferase and CCR5 expression vectors. Two different luciferase expression vectors were constructed. The first luciferase construct comprised HIV-1 Tat-regulated FL and the red fluorescent protein (DsRed) construct 53LTRN-lucneo^r#1. The HIV-1 Tat-responsive reporter construct 53LTRN-lucneo^r#1 was constructed based on the expression vector pGEM-7Zf(+) (Promega, Madison, WI). Initially, a parent vector was constructed, 53LTRNCNS, which has a rabbit β-globin unit under the control of the HIV-1 LTR derived from strain HXB2. In this construct, a gene of interest can be cloned within the second exon of the β-globin gene and the polyadenylation signal is provided by the β-globin unit. A neomycin expression module was prepared by PCR and cloned upstream of the HIV-1 LTR region to generate 53LTRCNSneo. The reporter gene employed here was a fusion between an FL gene and a DsRed gene. The FL gene allows HIV-1 replication to be quantitatively evaluated by using luciferase activity when the LTR is activated by HIV-derived Tat, and the DsRed gene allows transfected and HIV-infected cells to be identified by red fluorescence. The FL portion was derived from pGLuc5 (Promega), and the DsRed portion was derived from pDsRed1N-1 (Clontech). Both genes were prepared by PCR, fused, and cloned into the β-globin unit by using NcoI and NotI restriction sites.

The second luciferase construct, pRenillaPac, was constructed using the plasmid pPUR (Clontech). The PCR-amplified RL gene, derived from phRL-CMV (Promega), was spliced into the upstream region of the *pac* gene. This hybrid gene manifests both RL activity and resistance to puromycin. Expression of the fusion gene was constitutive under the control of a CMV promoter.

A CCR5 expression vector, pCCR5/CEP4, was constructed based on the pCEP4 expression vector (Invitrogen), which possesses the Epstein-Barr nuclear antigen 1 episomal-expression gene. The CCR5 gene was inserted into the vector by using NotI and SnaB I restriction sites on the vector. Expression of the CCR5 gene was constitutive under the control of a CMV promoter.

Selection of host cell line and establishment of new reporter cell lines. To design new reporter cell lines for quantifying HIV-1 replication, we selected the murine leukemia virus-transformed human T-cell line HPB-Ma, established by Y. K. Shimizu and H. Yoshikura (16, 29, 40), because of its high susceptibility to HIV-1 and its stable expression of CD4 and CXCR4. HPB-Ma cells were maintained at 37°C in 5% CO_2 in complete RPMI 1640 medium (Sigma, Tokyo, Japan) supplemented with 10% fetal calf serum (HyClone, Logan, UT) and 1% penicillin-streptomycin (Invitrogen, Tokyo, Japan). Cells were transfected by electroporation with the two luciferase expression vectors, 53LTRN-lucneo^r#1 and pRenillaPac. Plasmid DNA (10 μg) was mixed with HPB-Ma cells (5×10^6 cells in 500 μl phosphate-buffered saline), and the mixture was incubated for 5 min at 4°C and electropulsed with a Gene Pulser II apparatus (Bio-Rad, Hercules, CA) at 250 V and 950 μF. After electroporation, the cells were resuspended in complete medium and incubated at 37°C in 5% CO_2. Subsequently, cells with incorporated plasmids were selected with 0.1 μg/ml puromycin (BD Biosciences, San Jose, CA) and 250 μg/ml Geneticin (Invitrogen), maintained in complete medium for several weeks, and enriched with cell populations expressing high levels of CD4 and CXCR4 by fluorescence-activated cell sorting with a FACSVantage system (BD Biosciences). Finally, clones were generated by limiting dilution and selected if they showed high sensitivity to HIV-1 and low spontaneous expression of FL and DsRed.

Since the parent HPB-Ma cell line expresses only the CXCR4 receptor, we extended the spectrum of the reporter cell lines to include R5-tropic viral isolates by transfecting cells by electroporation with a CCR5 expression plasmid. Clones were selected by incubating for several weeks with 0.1 μg/ml puromycin, 250 μg/ml Geneticin, and 150 μg/ml hygromycin B. Selected cells were recloned, and the expression of cell surface markers was confirmed by using FACSCaliber (Becton Dickinson, San Jose, CA). CD4, CXCR4, and CCR5 receptors were stained with SK-3-Cy5.5, 12G5-phycoerythrin, and 2D7-fluorescein isothiocyanate monoclonal antibodies, respectively (all from BD Biosciences, San Jose, CA).

Evaluation of introduced reporter gene functions. To confirm the ability of FL activity to reliably measure virus titer and production, established cell lines were plated into 96-well plates at 10^5 cells per well and inoculated with 50 to 400 50% tissue culture infective doses ($TCID_{50}$) of HXB2 or JRCSF. After 7 days of culture with the test viruses, cells were harvested and lysed in 75 μl of luciferase assay reagent. FL activity was quantified using a Dual-Glo luciferase reporter assay system (Promega, Madison, WI) and an LMax microplate luminometer (Molecular Devices, Sunnyvale, CA). Virus production was also quantified by using the p24 antigen enzyme-linked immunosorbent assay RETROtek kit (ZeproMetrix Co., Buffalo, NY) and compared with FL activity.

The validity of using RL activity to monitor MaRBLE cell numbers was evaluated by measuring RL activity in various numbers of cells and determining the correlation between RL activity and cell numbers. The correlation between RL activity and cell viability was also confirmed in cell killing assays with two anticancer drugs, hygromycin B (Invitrogen, Tokyo, Japan) and blasticidin S (Funakoshi, Tokyo, Japan). Target cells were plated into 96-well plates at 10^5 cells per well, and hygromycin B (15.6 to 500 μg/ml) and blasticidin S (1.25 to 20 μg/ml) were added. After 7 days of culture, cells were harvested and RL activity was measured by using the Dual-Glo luciferase reporter assay system (Promega) and the percentage of cell killing was determined by trypan blue staining.

Preparation of recombinant and patient-derived viruses. Recombinant viruses with point mutations were constructed as described elsewhere (25). In brief, drug resistance mutations were introduced into the RT and protease genes of the HXB2 clone by site-directed mutagenesis (28). MT-2 cells (5×10^6 human T-lymphoblastoid cells) were then transfected by electroporation with the recombinant virus plasmids, and the cells were maintained in 10 ml of complete medium for 7 to 14 days. Half the culture supernatant was harvested and replaced with fresh medium every other day. Viral replication was monitored by measuring RT activity in the supernatant, and the sample with the highest RT activity was used in subsequent studies.

Eight clinical samples were selected randomly from patient blood specimens sent for routine HIV-1 drug resistance testing to the AIDS Research Center, National Institute of Infectious Diseases, Tokyo, Japan. Patient viruses were isolated by a standard coculture method described elsewhere (18). In brief, 2×10^7 patient PBMC were mixed with the same number of phytohemagglutinin-stimulated normal human PBMC and the mixture was cultured for 2 weeks. Half the culture supernatant was collected and replaced with the same amount of fresh culture medium every other day. Viral replication was monitored by mea-

suring RT activity in the supernatant, and the sample with peak RT activity was selected and used for infection experiments afterward. RT assays were performed as previously described (37). Viral RNAs in collected supernatants were sequenced, and drug resistance mutation patterns were determined.

For the reconstructed virus, viral RNA was extracted from 200 μl of patient plasma by using a High Pure viral RNA kit (Roche, Basel, Switzerland) according to the manufacturer's instructions. Subsequently, a 1.8-kb *gag-pol* fragment, encoding the region from $p2^{SP2}$ to whole protease, and the 5′ half of the RT gene fragment were amplified and inserted into the HXB2 backbone. MT-2 cells (5×10^6) were then transfected by electroporation with the plasmid, and the cells were maintained in 10 ml of complete medium for 7 to 14 days. Half the culture supernatant was harvested and replaced with fresh medium every other day. Viral replication was monitored by measuring RT activity in the supernatant, and the sample with the highest RT activity was selected for use in subsequent studies. Viral RNAs in collected supernatants were sequenced, and the drug resistance mutation patterns were confirmed. For both the patient-derived and reconstructed viruses, HIV infectivity ($TCID_{50}$) in the target cell lines was assayed by the Reed-Muench method (27).

Drug resistance genotyping. HIV-1 RNA was extracted from 200 μl of patient plasma using a High Pure viral RNA kit according to the manufacturer's instructions. For amplification of the 500-bp protease gene fragment, DRPRO5 (5′-AGA-CAG-GYT-AAT-TTT-TTA-GGG-A) and DRPRO2L (5′-TAT-GGA-TTT-TCA-GGC-CCA-ATT-TTT-GA) were used for reverse transcription and the first PCR and DRPRO1M (5′-AGA-GCC-AAC-AGC-CCC-ACC-AG) and DRPRO6 (5′-ACT-TTT-GGG-CCA-TCC-ATT-CC) were used for the second PCR. For amplification of the 800-bp RT gene fragment, DRRT1L (5′-ATG-ATA-GGG-GGA-ATT-GGA-GGT-TT) and DRRT4L (5′-TAC-TTC-TGT-TAG-TGC-TTT-GGT-TCC) were used for reverse transcription and the first PCR and DRRT7L (5′-GAC-CTA-CAC-CTG-TCA-ACA-TAA-TTG-G) and DRRT6L (5′-TAA-TCC-CTG-CAT-AAA-TCT-GAC-TTG-C) were used for the second PCR. The amplicons were purified by using a MultiScreen PCR filter plate (Millipore), and sequence reactions were performed by using the BigDye Terminator v3.1 cycle sequencing kit, followed by electrophoresis using an ABI-3730 auto sequencer (Applied Biosystems, Foster City, CA).

HIV-1 replication kinetics analyses and drug susceptibility assays. To analyze the replication kinetics of clinically derived HIV-1 isolates, target cells were plated into 96-well plates at 10^5 cells per well and infected with 100 $TCID_{50}$ of test viruses per well. At days 3, 5, and 7, the culture supernatant of each well was collected and RT activity was measured as previously described (37).

To evaluate anti-HIV-1 drug susceptibility, 10^7 cells were infected with 10,000 $TCID_{50}$ of wild-type control or test viruses in 50-ml tubes and incubated for 2 h at 37°C. Infected cells were resuspended in culture medium and plated into 96-well plates at 10^5 cells per well. At 2 and 48 h after infection, serial RT inhibitor dilutions and serial protease inhibitor (PI) dilutions were added, respectively. Each drug was prepared in a fivefold serial dilution and tested over different dose ranges, as follows. Didanosine, abacavir, and nevirapine were tested at concentrations from 25.0×10^1 μm to 3.2×10^{-4} μM. Lamivudine and stavudine were tested at concentrations from 5.0×10^1 μm to 6.4×10^{-5} μM. Zidovudine, zalcitabine, and the five PIs (saquinavir, indinavir, nelfinavir, lopinavir, and amprenavir) were tested at concentrations from 1.0×10^1 μm to 12.8×10^{-6} μM. Efavirenz was tested at concentrations from 0.2×10^1 μm to 25.6×10^{-7} μM. All samples were tested in triplicate. The following manufacturers kindly supplied anti-HIV drugs: GlaxoSmithKline, Middlesex, United Kingdom (zidovudine, lamivudine, and abacavir); Bristol-Myers Squibb, New York, NY (didanosine, stavudine, and efavirenz); Roche, Basel, Switzerland (zalcitabine and saquinavir); Boehringer Ingelheim, Ingelheim, Germany (nevirapine); Merck Research Laboratories, Rahway, NJ (indinavir); Japan Tobacco, Tokyo, Japan (nelfinavir); Vertex Pharmaceuticals, Cambridge, MA (amprenavir); and Abbott Laboratories, Abbott Park, IL (lopinavir).

After 7 days of culture with test drugs and test viruses, cells were harvested and lysed in 75 μl of luciferase assay reagent. Firefly and RL activities were sequentially quantified using a dual-luciferase reporter assay system (Promega) and an LMax microplate luminometer (Molecular Devices). Data were displayed by plotting the percentage of luciferase activity versus the $\log_{10}$ drug concentration. The concentration at which 50% of viral replication was inhibited (IC_{50}) was determined by plotting curves defined by the four-parametric sigmoidal equation $f(x) = A + ([B - A])/(1 + [C/x]^D)$ using XLfit4 software (CTC Laboratory Systems Corporation, Tokyo, Japan). To determine susceptibility or resistance, results for test viruses were compared to those for wild-type HIV-1 and evaluated by Student's *t* test.

RESULTS

Establishment of new T-cell-based cell lines with two luciferase reporter proteins. Two luciferase expression vectors were successfully constructed and used for transfection of the HPB-Ma cell line. These vectors were 53LTRN-lucneo^r#1, with FL under HIV-1 LTR regulation, and pRenillaPac, with RL under CMV promoter regulation. HPB-Ma cells with these vectors were subjected to several rounds of selection for cells resistant to Geneticin and puromycin and were enriched by flow cytometry with populations expressing high levels of CD4 and CXCR4 to establish the new cell line HPB-Ma/LTR-FL/CMV-RL (X4-MaRBLE).

Since the parent HPB-Ma cell line expresses only CXCR4, the spectrum of the X4-MaRBLE cell line was extended to include R5-tropic viruses by transfection with a CCR5 expression plasmid, thus establishing the R5-MaRBLE cell line. Expression levels of CD4 were comparable among the parent HPB-Ma, X4-MaRBLE, and R5-MaRBLE cell lines (Fig. 1a to c), whereas the proportion of CXCR4-positive cell populations and CXCR4 expression levels were slightly higher in X4- and R5-MaRBLE cells than in the parent HPB-Ma cell line (Fig. 1d to f). This difference is due to the cell sorter's selecting for populations expressing high levels of CXCR4. As for CCR5 expression, HPB-Ma and X4-MaRBLE cells did not significantly express the receptor (Fig. 1g and h). On the other hand, more than 76% of the R5-MaRBLE cell population expressed CCR5 (Fig. 1i).

To confirm the susceptibility of cell lines to X4- and R5-tropic viruses, each cell line was inoculated with HXB2 (X4-tropic) and JRCSF (R5-tropic) viruses. X4-MaRBLE cells inoculated with HXB2 expressed FL activity in a dose-dependent manner but did not show any FL activity after inoculation with JRCSF (Fig. 2a). On the other hand, R5-MaRBLE cells were susceptible to both HXB2 and JRCSF, which induced FL activity in a dose-dependent manner (Fig. 2b). To validate the use of FL activity to evaluate viral production, FL levels were compared to amounts of the viral capsid antigen, p24, in both X4- and R5-MaRBLE cell lines, and the correlation between FL levels and the amounts of p24 was determined. As shown in Fig. 2c, FL activity in cell lysates and the amount of p24 antigen in the culture supernatant were positively and linearly correlated in X4-MaRBLE cells infected with HXB2 ($r^2 = 0.98$), in R5-MaRBLE cells infected with HXB2 ($r^2 = 0.91$), and in R5-MaRBLE cells infected with JRCSF ($r^2 = 0.94$). These results verify that FL activity expressed by both X4- and R5-MaRBLE cell lines accurately represents the levels of viral replication and production. These good correlations also indicate a small likelihood of interference between the two LTRs in infected cells, the one driving luciferase and the other contained in the infecting virus.

The second type of luciferase, RL, was inserted into MaRBLE cells to monitor and evaluate their number and viability. As shown in Fig. 3a, RL activity demonstrated a positive, linear correlation with cell number ($r^2 = 0.99$). Thus, RL activity can be used to assess cell number in culture. Another useful parameter evaluated by RL activity was the cytotoxicity of test compounds added to cultures. To confirm the relationship between RL activity and cell viability, cell killing assays were performed with two anticancer drugs, hygromycin

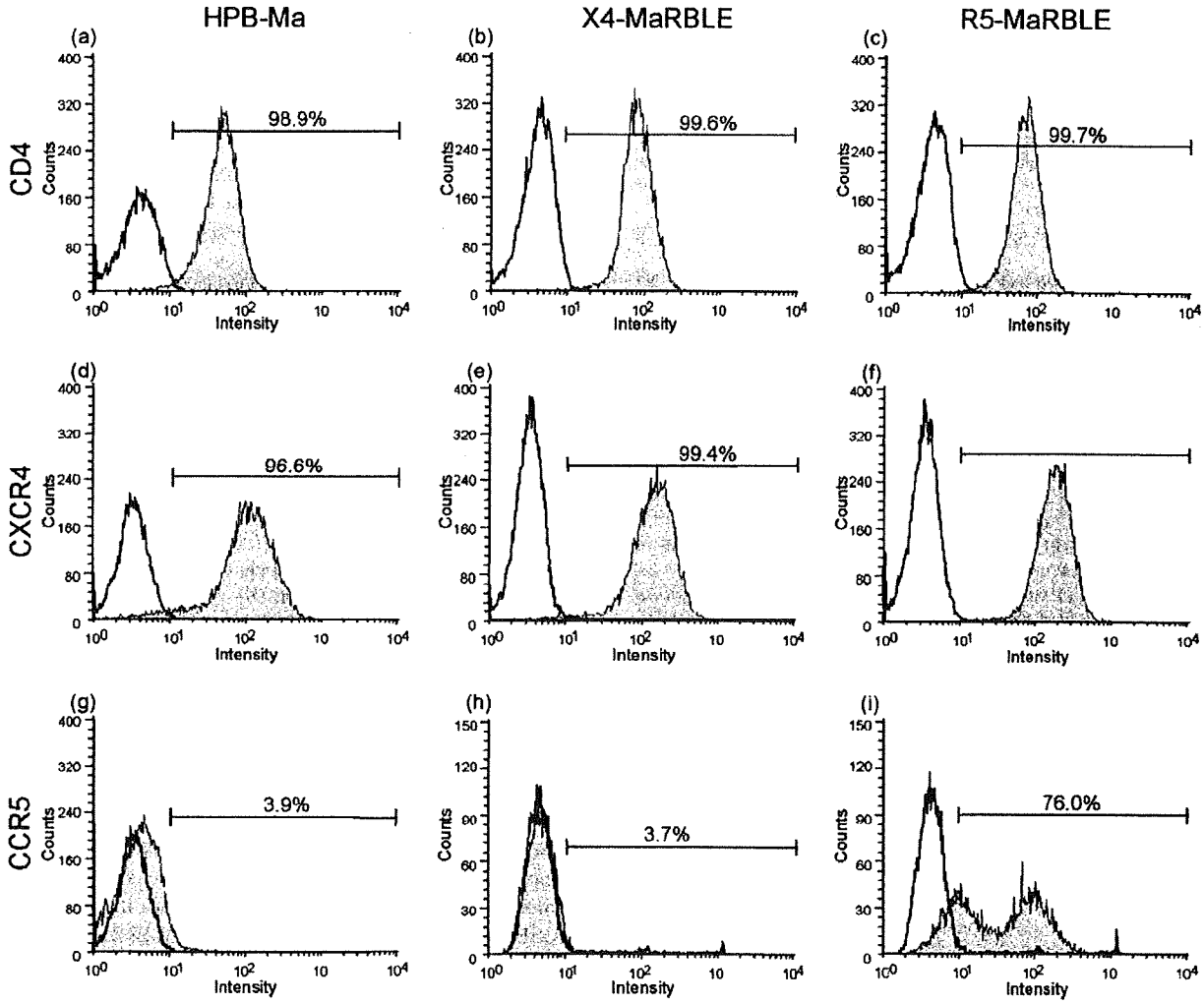

FIG. 1. Levels of expression of CD4, CXCR4, and CCR5 in parent HPB-Ma cells and X4-MaRBLE and R5-MaRBLE cells. Parent HPB-Ma (a, d, g), X4-MaRBLE (b, e, h), and R5-MaRBLE (c, f, i) cells were stained with monoclonal antibodies to CD4 (a, b, c), CXCR4 (d, e, f), and CCR5 (g, h, i). To calculate the percentage of each population positive for the expression of cytokine receptors (bars), 2,000 to 5,000 cells were analyzed by fluorescence-activated cell sorting. To calculate the percentage of each population positive for expression of CD4 and cytokine receptors (bar), 2,000 to 5,000 cells were analyzed by FACSCalibur and compared with fluorescence-negative control cells. Histograms with gray shading indicate cell populations stained with each monoclonal antibody; histograms without shading indicate negative control populations.

B (Fig. 3b) and blasticidin S (Fig. 3c). As the percentages of cells killed by both test chemicals increased, RL activity declined (Fig. 3b and c). The concentrations of hygromycin B and blasticidin S needed to kill 50% of the cells were 100 μg/ml and 2 μg/ml, respectively, in agreement with data from previous reports (3, 32). Thus, RL activity can be used to measure cytotoxicity.

In addition, the replication of two patient-derived viral isolates, 8 and 9, in R5-MaRBLE cells was compared to that in PBMC. As shown in Fig. 4, the two clinical isolates efficiently replicated in R5-MaRBLE cells. Isolate 8 replicated more efficiently in R5-MaRBLE cells than in PBMC, as indicated by the 10-fold-higher RT activity at day 7 in R5-MaRBLE cells (Fig. 4a). Isolate 9 had comparable day 7 RT activities in R5-MaRBLE cells and PBMC (Fig. 4b). These data clearly show that R5-MaRBLE cells can efficiently propagate clinical isolates.

Evaluation of HIV-1 drug susceptibility using X4- and R5-MaRBLE cells is highly reproducible. Having confirmed the quantitative reliability of FL expressed by HIV-infected X4- and R5-MaRBLE cell lines, we next used the cell lines to evaluate HIV-1 susceptibility to antiretroviral drugs. First, we evaluated the precision of phenotyping using the X4- and R5-MaRBLE cell lines. By using the wild-type HXB2 strain as a target virus for both X4- and R5-MaRBLE cells and JRCSF as a target virus for R5-MaRBLE cells, the IC_{50}s of four representative drugs from three classes of antiretroviral agents (zidovudine, lamivudine, efavirenz, and lopinavir) were determined by measuring FL activity. As shown in Fig. 5, well-characterized dose-response curves were obtained for the four drugs. The mean IC_{50}s, standard deviations (SD), and coefficients of variation (CV) for each cell line are summarized in Table 1. The CV ranged from 17 to 41%, demonstrating high reproducibility for drug susceptibility assays using both HIV-

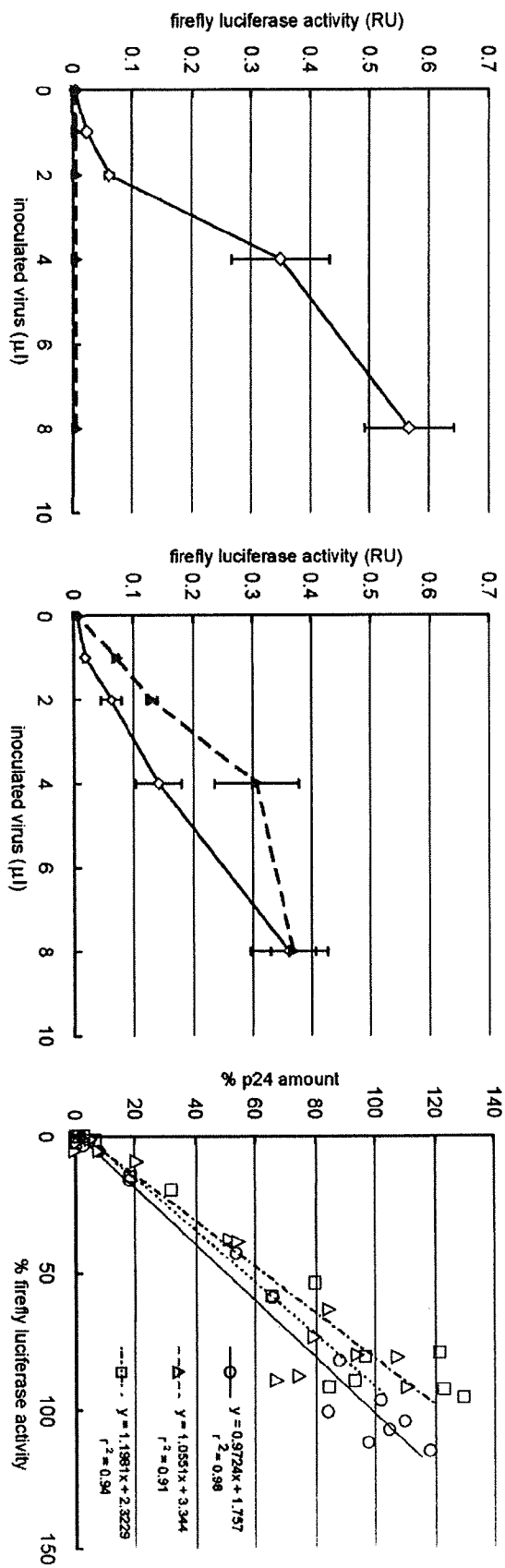

FIG. 2. FL reporter activity in MaRBLE cells accurately represents viral production\chatn. (a) X4-MaRBLE cells are susceptible to HXB2 (X4-tropic) but not JRCSF (R5-tropic) viruses. FL activity was confirmed as a reliable measure of X4-tropic HIV-1 in X4-MaRBLE cells by inoculating the cells with various amounts of HXB2 or JRCSF and reading FL activity 7 days later. Solid and dashed lines indicate HXB2 and JRCSF, respectively. (b) R5-MaRBLE cells are susceptible to both HXB2 (X4-tropic) and JRCSF (R5-tropic) viruses. FL activity was confirmed as a reliable measure of X4- and R5-tropic HIV-1 in R5-MaRBLE cells by inoculating the cells with various amounts of HXB2 or JRCSF and reading FL activity 7 days later. Solid and dashed lines indicate HXB2 and JRCSF, respectively. (c) FL activity and the amount of capsid antigen p24 are correlated in HIV-infected MaRBLE cells. The reliability of using FL activity instead of the amount of p24 to quantify HIV-1 production was evaluated by measuring intracellular FL activity and the amount of p24 antigen in the supernatant from the same culture. Solid, dashed, and dotted lines indicate HXB2-infected X4-MaRBLE cells, HXB2-infected R5-MaRBLE cells, and JRCSF-infected R5-MaRBLE cells, respectively. Percentages of FL activity and of p24 production were calculated from the following formula: percentage = (observed value with the drug − background value)/(observed value without the drug − background value) × 100. RU, relative units.

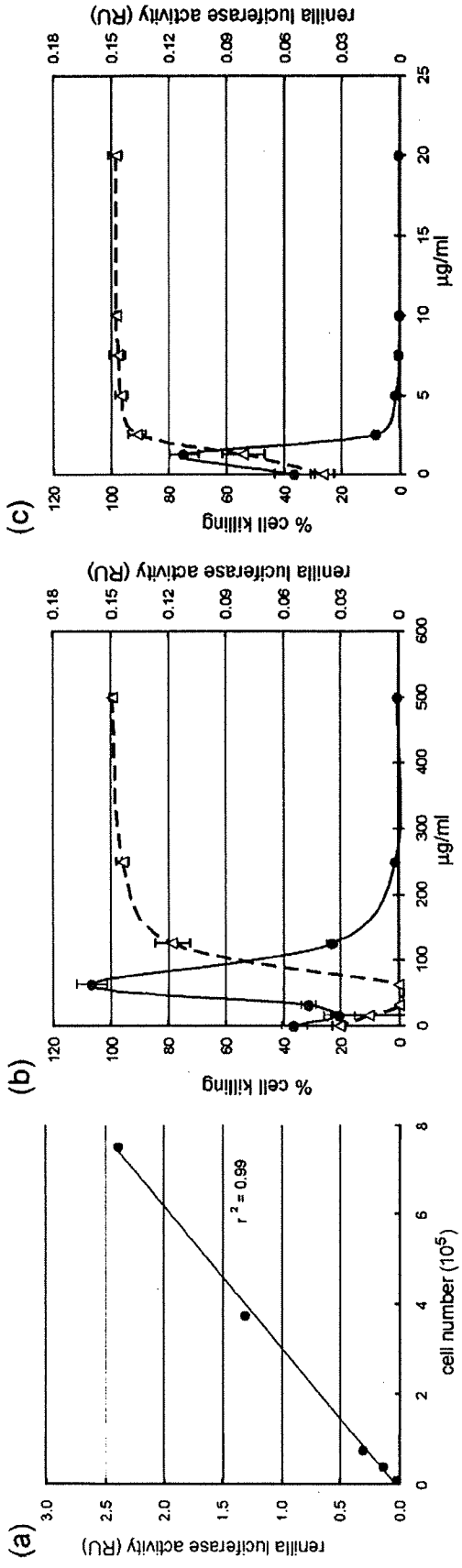

FIG. 3. Constitutively expressed RL in MaRBLE cells provides a reliable measure of cell number and viability. (a) RL activity accurately indicates MaRBLE cell numbers. The validity of using RL activity to monitor MaRBLE cell numbers was evaluated by measuring RL activity in various numbers of cells and plotting the corresponding values. RL activity and cell number were positively and linearly correlated ($r^2 = 0.99$). (b and c) RL activity reliably indicates hygromycin B and blasticidin S cytotoxicity in MaRBLE cells. The reliability of RL activity as a marker of cytotoxicity was evaluated for hygromycin B (b) and blasticidin S HCl (c). Cells were cultured for 1 week with serial dilutions of each drug and lysed, and their RL activities were determined. In graphs in both panels b and c, solid lines represent the RL activities of cell lysates and dashed lines indicate percentages of dead cells as determined by trypan blue staining. RU, relative units.

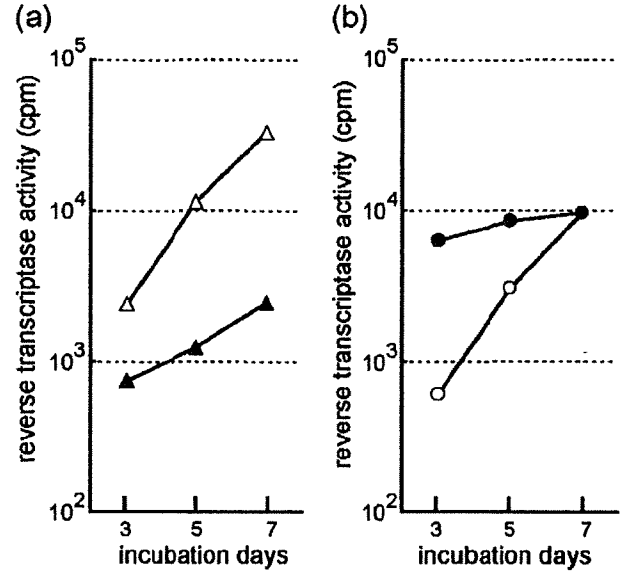

FIG. 4. Clinically derived isolates replicate in R5-MaRBLE cells as efficiently as in PBMC. The replication kinetics of two clinical isolates, 8 and 9, were compared after inoculation into both R5-MaRBLE cells and human PBMC. (a) Replication kinetics of isolate 8. Open and closed triangles indicate kinetics in R5-MaRBLE cells and PBMC, respectively. (b) Replication kinetics of isolate 9. Open and closed circles indicate kinetics in R5-MaRBLE cells and PBMC, respectively. cpm, counts per minute.

1-inoculated X4- and R5-MaRBLE cells. Interestingly, while the efavirenz and lopinavir susceptibilities of wild-type HXB2 were identical in evaluations with both X4- and R5-MaRBLE cells, the IC_{50}s for HXB2 and JRCSF were significantly different ($P < 0.001$) in the R5-MaRBLE cell line. Thus, in our assay, JRCSF appeared to be more susceptible than the HXB2 HIV-1 strain to efavirenz and slightly less resistant to lopinavir.

Drug susceptibility of drug-resistant HIV-1 can be evaluated using X4- and R5-MaRBLE cell lines. Given the accuracy and reproducibility of assays using MaRBLE cells to determine the drug susceptibilities of wild-type HXB2 and JRCSF, we then evaluated the reliability of using the cell lines for drug resistance phenotyping. Recombinant viruses with representative drug resistance mutations were constructed, and the drug resistance levels of the viruses were determined using X4-MaRBLE cells. The drug resistance levels associated with five patterns of nucleoside RT inhibitor (NRTI) resistance mutations are summarized in Table 2. Of the five mutant viral clones tested, four showed significant resistance to zidovudine, with resistance levels in the following order from lowest to highest: M41L/M184V/T215Y ≤ D67N/K70R < M41L/T215Y < M41L/D67N/K70R/T215Y. Thus, zidovudine resistance increased with the accumulation of thymidine analogue mutations (TAMs), and the M184V mutation caused reversion to the zidovudine resistance phenotype in the M41L/T215Y mutant, with a change in the susceptibility level of 12.5- to 3.5-fold relative to that of the wild-type virus, similar to results in previous reports (11, 19). Two clones with the M184V mutation demonstrated over 500-fold (>533.7- and >1,339.3-fold)-greater resistance to lamivudine but no significant resistance to didanosine and zalcitabine, although M184V has been re-

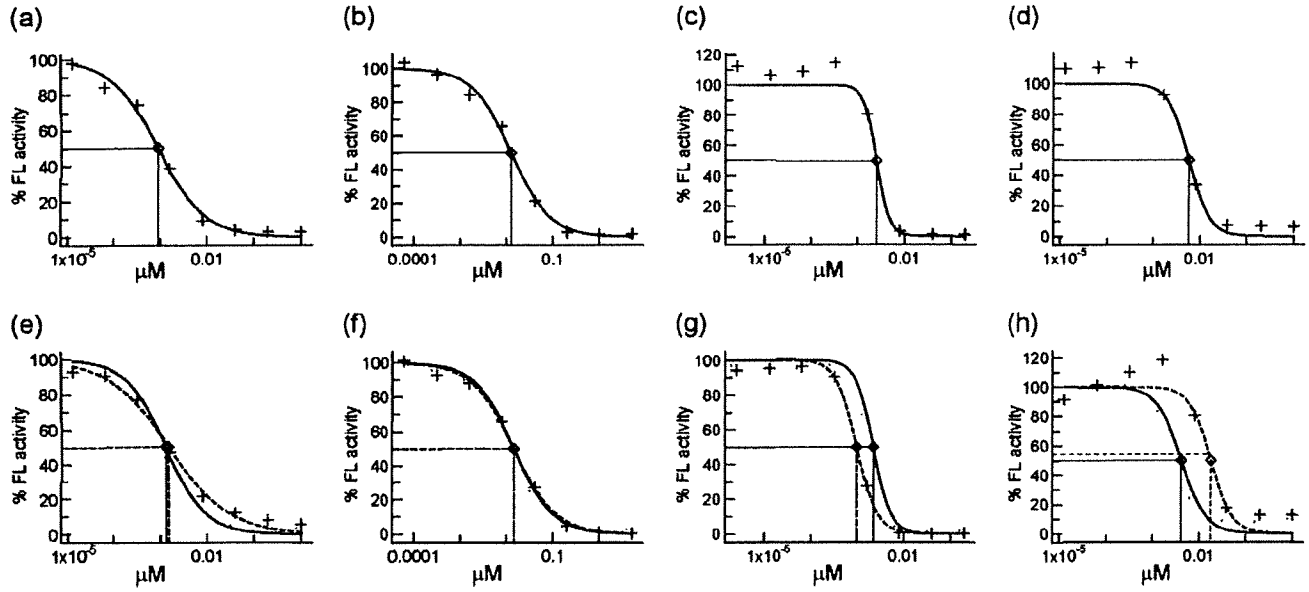

FIG. 5. Results of assays for HIV-1 drug susceptibility with MaRBLE reporter cell lines are highly reproducible. Dose-response curves for four representative agents against wild-type HXB2 and JRCSF are shown. Solid and dotted lines indicate HXB2 and JRCSF, respectively. (a to d) Results of assays for susceptibility to zidovudine, lamivudine, efavirenz, and lopinavir, respectively, using X4-MaRBLE cells. (e to h) Results of assays for susceptibility to zidovudine, lamivudine, efavirenz, and lopinavir, respectively, using R5-MaRBLE cells. The percentage of inhibition was calculated as follows: percentage = (observed FL activity with the drug − background FL activity)/(FL activity without the drug − background FL activity) × 100.

ported to confer a three- to fivefold increase in the level of resistance (14). Our data confirm the recent revalidation of using didanosine for cases involving the M184V mutation (39). Low-level but significant stavudine resistance in M41L/T215Y (change, 2.2-fold), M41L/M184V/T215Y (change, 2.9-fold), and M41L/D67N/K70R/T215Y (change, 3.8-fold) was found, consistent with data from previous reports (22, 33). All five clones demonstrated significant resistance to abacavir. The highest resistance was observed in the M41L/M184V/T215Y mutant, consistent with findings in previous reports that TAMs with M184V reduce susceptibility to abacavir 10-fold (1).

The drug resistance levels associated with the two most common nonnucleoside RT inhibitor (NNRTI) resistance mutations (K103N and Y181C) are summarized in Table 3. The K103N mutant virus demonstrated reduced susceptibility to both nevirapine (change, 78.6-fold) and efavirenz (change, 54.7-fold), whereas the Y181C virus was resistant only to nevirapine (change, 47.5-fold) but remained susceptible to efavirenz (change, 1.5-fold).

TABLE 1. Susceptibility of wild-type HXB2 and JRCSF to representative antiretrovirals as determined using X4- and R5-MaRBLE cells

Cell line	Agent	Mean IC_{50} (nM) ± SD (CV [%]) for[a]: HXB2 (n = 18)	HXB2 (n = 21)	JRCSF (n = 24)
X4-MaRBLE	Zidovudine	0.9 ± 0.4 (41)		
	Lamivudine	12.3 ± 3.9 (32)		
	Efavirenz	2.7 ± 1.0 (37)		
	Lopinavir	6.0 ± 1.0 (17)		
R5-MaRBLE	Zidovudine		1.3 ± 0.4 (31)	1.5 ± 0.6 (40)
	Lamivudine		13.6 ± 4.8 (35)	13.4 ± 3.6 (27)
	Efavirenz		2.1 ± 0.5[b] (24)	1.0 ± 0.3[b] (30)
	Lopinavir		4.2 ± 1.4[b] (33)	17.6 ± 6.9[b] (39)

[a] n, number of isolates of the indicated virus strain.
[b] IC_{50}s of efavirenz and lopinavir were significantly different for HXB2 and JRCSF in R5-MaRBLE cells ($P < 0.001$).

To assess the reliability of using R5-MaRBLE cells to evaluate the levels of drug resistance of viral isolates from patients for whom treatment failed, seven cases were selected and viruses were isolated by coculture with normal human PBMC. Among the isolates from these seven cases, isolate 7 did not yield measurable virus by coculture. Therefore, a protease-RT gene fragment was amplified by RT-PCR and inserted into the HXB2 backbone. As shown in Table 5, isolate 1 had three minor mutations in the protease region and the virus was susceptible to all four inhibitors tested. The increase in resistance, calculated by comparison to the drug resistance of JRCSF, was <1.0-fold for zidovudine, lamivudine, and lopina-

The drug resistance levels of three PI-resistant mutant clones (M46I, V82T, and L90M) are summarized in Table 4. Clones with M46I and L90M mutations did not demonstrate significant resistance to any PI tested, except for nelfinavir, to which the L90M clone demonstrated low-level (change, 3.3-fold) resistance. The clone with the V82T mutation demonstrated low-level resistance to indinavir (change, 3.8-fold), nelfinavir (change, 5.4-fold), amprenavir (change, 2.9-fold), and lopinavir (change, 5.0-fold), consistent with results in previous reports (8). Thus, the drug susceptibilities of viruses with resistance mutations evaluated with the MaRBLE cell lines matched those from previous reports of drug resistance, indicating the reliability of using the new cell lines to evaluate drug resistance.

TABLE 2. Drug resistance levels associated with NRTI resistance mutations as determined using X4-MaRBLE cells infected with HIV-1 clones

Agent	IC_{50} (nM) ± SD (change, *n*-fold)[a] for:					
	Wild type	M41L/T215Y	M184V	M41L/M184V/T215Y	D67N/K70R	M41L/D67N/K70R/T215Y
Zidovudine	0.8 ± 0.4	10.6 ± 6.9[c] (12.5 ± 1.9)	0.4 ± 0.1 (0.5 ± 0.01)	1.9 ± 1.0[b] (3.5 ± 0.5)	4.6 ± 1.0[c] (4.6 ± 1.2)	54.0 ± 32.3[c,d,e] (48.1 ± 16.0)
Didanosine	2,097.7 ± 1,101.4	2,899.8 ± 1,627.9 (1.4 ± 0.4)	2,164.6 ± 1,019.8 (1.3 ± 0.2)	2,893.7 ± 1519.0 (2.1 ± 0.8)	3,754.2 ± 1,468.3 (1.4 ± 0.3)	5,082.9 ± 2,397.5[b] (1.8 ± 0.5)
Zalcitabine	2.5 ± 1.1	3.8 ± 3.3 (1.5 ± 0.8)	3.4 ± 0.6 (1.3 ± 0.4)	3.9 ± 2.0 (2.2 ± 0.8)	3.0 ± 0.8 (1.2 ± 0.3)	3.5 ± 2.3 (1.2 ± 0.6)
Lamivudine	8.7 ± 4.5	20.9 ± 14.5[b] (3.8 ± 3.2)	>5,000[c] (>533.7)	>5,000[c] (>1,339.3)	17.8 ± 6.9[b] (2.4 ± 1.3)	44.3 ± 27.7[c] (6.8 ± 7.4)
Stavudine	14.4 ± 5.2	29.9 ± 14.0[b] (2.2 ± 0.4)	17.5 ± 7.6 (0.9 ± 0.3)	40.7 ± 23.8[b] (2.9 ± 1.1)	31.3 ± 24.9 (2.3 ± 1.7)	50.3 ± 24.2[c] (3.8 ± 1.6)
Abacavir	348.7 ± 122.8	985.5 ± 306.3[c] (3.2 ± 1.1)	1,497.5 ± 589.4[c] (3.9 ± 1.2)	3,300.0 ± 1,986.9[c,d] (10.6 ± 3.1)	836.2 ± 522.5[b] (2.1 ± 0.7)	2,015.1 ± 842.8[c,d] (5.2 ± 0.9)

[a] Change (*n*-fold) = (observed IC_{50} for strain)/(IC_{50} for wild type).
[b] P, <0.05 for comparison with wild-type virus.
[c] P, <0.005 for comparison with wild-type virus.
[d] P, <0.05 for comparison with M41L/T215Y virus.
[e] P, <0.05 for comparison with D67N/K70R virus.

vir. The patient in case 2 had been heavily treated with antiretroviral agents, and isolate 2 had a high accumulation of NRTI and PI resistance mutations but no NNRTI resistance mutation. This isolate had six TAMs and an M184V mutation in the RT region and demonstrated resistance to zidovudine (change, 32.9-fold) and lamivudine (change, >380.7-fold) but not to efavirenz. As for the protease region, 11 mutations were detected, including three major mutations (M46I, V82F, and L90M). Of these 11 mutations, 10 matched known lopinavir resistance mutations (International AIDS Society—USA drug resistance chart) (20). Indeed, high resistance to lopinavir (change, >76.5-fold) was observed.

Isolate 3 had 6 TAMs (M41L, E44D, D67N, V118I, L210W, and T215Y), and a high level of resistance to zidovudine (change, 114.5-fold) was observed. As the virus in this isolate had all four known NRTI resistance mutations responsible for hypersusceptibility to NNRTIs, it was hypersusceptible to efavirenz (change, 0.2-fold). Efavirenz hypersusceptibility was defined as a change in resistance of <0.4-fold compared to that of the wild type by statistical analysis (mean value minus 2 SD) and by data from a previous report (4). Isolate 4 had accumulated five TAMs and demonstrated 191.7-fold-higher resistance to zidovudine. No lamivudine resistance and NNRTI resistance mutations were observed, and the virus was susceptible to lamivudine. Isolate 4 also had M41L, V118I, L210W, and T215Y mutations, and the virus demonstrated hypersusceptibility to efavirenz (change, 0.2-fold). Two major mutations, D30N and L90M, and eight secondary mutations in the protease region were observed. Of these eight secondary mutations, five matched lopinavir resistance mutations, with our assay indicating a 9.4-fold increase in resistance to lopinavir. Isolate 5 had an RT inhibitor resistance pattern similar to that of isolate 2, having accumulated six TAMs and the M184V lamivudine resistance mutation in RT and demonstrating 104.1-fold-higher resistance to zidovudine and >380.7-fold-higher resistance to lamivudine. This virus also had M41L, V118I, L210W, and T215Y mutations. Though this virus appeared to be slightly more susceptible to efavirenz (change, 0.6-fold), this effect was not statistically significant. Isolate 5 had accumulated 11 lopinavir resistance mutations in the protease region and demonstrated 75.5-fold-higher resistance to lopinavir in our assay.

Isolate 6 had accumulated six TAMs in RT and showed 224.0-fold-higher resistance to zidovudine. This isolate had E44D and V118I mutations (low-level-lamivudine-resistance mutations) and showed 6.7-fold-higher resistance to lamivudine. Similar to those in cases 3 to 5, the virus in case 6 had M41L, V118I, L210W, and T215Y mutations and demonstrated slight hypersusceptibility to efavirenz (change, 0.4-fold). As for the protease region, isolate 6 had three major mutations, M46I, I84V, and L90M, and six minor resistance mutations. Of these nine mutations, eight were listed as lopinavir resistance mutations, and intermediate-level resistance to lopinavir (change, 14.6-fold) was observed. Isolate 7R had K103N and showed high-level resistance to efavirenz (change, 66.8-fold). No other drug resistance mutations in the RT region were found, and thus the isolate was susceptible to zidovudine and lamivudine. The protease region did show two minor mutations, L63C and V77I, and the isolate was susceptible to lopinavir.

TABLE 3. Drug resistance levels associated with NNRTI resistance mutations as determined using X4-MaRBLE cells infected with HIV-1 clones

Agent	IC_{50} (nM) ± SD (change, *n*-fold)[a] for:		
	Wild type	K103N	Y181C
Nevirapine	206.3 ± 68.2	16,110.7 ± 6,445.7[b] (78.6 ± 19.7)	9,586.3 ± 6,396.4[c] (47.5 ± 23.8)
Efavirenz	1.4 ± 0.4	79.3 ± 33.3[b] (54.7 ± 15.6)	2.3 ± 0.6[c] (1.5 ± 0.1)

[a] Change (*n*-fold) = (observed IC_{50} for strain)/(IC_{50} for wild type).
[b] *P*, <0.005 for comparison with wild-type virus.
[c] *P*, <0.05 for comparison with wild-type virus.

Thus, the increases observed in levels of resistance to zidovudine and lopinavir were associated with the accumulation of known resistance mutations associated with those drugs. Similarly, hypersusceptibility to efavirenz was associated with the accumulation of M41L, V118I, L210W, and T215Y mutations in four out of six clinical isolates (30). Taken together, these results confirm the reliability of using X4- and R5-MaRBLE cells in drug resistance phenotyping.

DISCUSSION

The development of reliable methodologies to evaluate drug susceptibility in vitro has been a major thrust of drug resistance research. Although several phenotypic assays are commercially available for clinical usage, they are expensive and may not be readily available either in developing or developed countries. As for use in research laboratories, these commercial assays target only the protease and reverse transcriptase gene regions of the HIV-1 genome, limiting their flexibility as a tool for basic research. Thus, there is still a need for easy-to-use assay systems with high reproducibility, for both clinical and research usage. To fill this gap, we drew a blueprint for a new type of reporter cell line by considering the advantages and drawbacks of several previously reported cell lines (12, 15, 17, 21, 24, 26, 31, 36). Based on this blueprint, we chose the T-cell-based cell line HPB-Ma (16, 29, 40) as the parent cell line to introduce reporter genes and to establish new reporter cell lines. HPB-Ma is a murine leukemia virus-transformed human T-cell line demonstrating high susceptibility to HIV-1, which can replicate efficiently in these host cells. As HPB-Ma cells naturally express CD4 and CXCR4, but not CCR5, we introduced the CCR5 expression gene to widen the susceptibility spectrum of the cell line to include R5-tropic viruses. The reporter protein chosen to measure HIV infectivity was FL, as it has a wider dynamic range than other known reporter candidates. Another type of luciferase, RL, was introduced as a marker of cell number and viability.

Finally, two types of new reporter cell lines were established, X4-MaRBLE and R5-MaRBLE. As expected, these new cell lines had several advantages over previously described cell lines. First, viruses efficiently propagated in these cell lines, making multiple-round replication assays possible. In addition, viruses could be isolated from patient plasma and PBMC by using the cell lines. Since other reporter cells may not allow replication-competent viruses to be efficiently produced, their use is largely limited to single-cycle replication assays. These assays are currently accepted as the major method for measuring viral infectivity due to their rapid readout of results. However, single-cycle replication assays cannot evaluate the postintegration late phase of the viral life cycle. To evaluate late-phase inhibitors, such as PIs, by using single-cycle replication assays, an additional step is required prior to the assay to produce viruses under test drug pressure. On the other hand, multiple-round replication assays allow late-phase inhibitors to be directly evaluated, just as early-phase inhibitors, without additional culture. Furthermore, multiple-round replication assays allow for a clearer readout of drug susceptibility, as the differences in drug susceptibilities between the reference and test viruses may be amplified by each round of replication.

Second, the cell lines were successfully transfected with RL to broaden their application. The constitutive expression of this second luciferase in the cell line has made it possible to easily and accurately evaluate cell number and the cytotoxicities of test compounds. As we planned to conduct multiple rounds of assays, the cells were cultured for at least a week, long enough for them to propagate and increase the background level of FL. The extent of this increase depended on the amount of viral inocula or the level of inhibition by antiretroviral agents. By monitoring RL activity,

TABLE 4. Drug resistance levels of PI-resistant mutants analyzed using HIV-1-infected X4-MaRBLE cells

Agent	IC_{50} (nM) ± SD (change, *n*-fold)[a] for:			
	Wild type	M46I	V82T	L90M
Indinavir	11.3 ± 4.3	19.5 ± 17.0 (2.2 ± 2.7)	38.0 ± 6.8[b] (3.8 ± 1.6)	11.5 ± 1.5 (1.1 ± 0.3)
Saquinavir	7.4 ± 3.4	5.0 ± 2.4 (0.7 ± 0.3)	6.5 ± 1.3 (1.0 ± 0.4)	6.9 ± 1.1 (1.0 ± 0.4)
Nelfinavir	4.9 ± 2.3	7.4 ± 5.3 (1.9 ± 1.5)	20.0 ± 5.5[b] (5.4 ± 3.7)	11.5 ± 0.7[d] (3.3 ± 2.2)
Amprenavir	6.7 ± 3.1	9.7 ± 5.4 (2.0 ± 2.0)	17.2 ± 5.2[c] (2.9 ± 1.0)	10.7 ± 2.1 (2.0 ± 1.3)
Lopinavir	6.6 ± 3.8	6.3 ± 2.9 (1.1 ± 0.7)	29.1 ± 9.0[c] (5.0 ± 1.8)	5.6 ± 0.9 (1.1 ± 0.7)

[a] Change (*n*-fold) = (observed IC_{50} for strain)/(IC_{50} for wild type).
[b] *P*, <0.005 for comparison with wild-type virus.
[c] *P*, <0.05 for comparison with wild-type virus.
[d] *P*, <0.01 for comparison with wild-type virus.

TABLE 5. Susceptibilities of seven patient-derived viral isolates to representative drugs assayed using R5-MaRBLE cells

Strain or isolate (subtype)	Tropism[b]	RT mutation(s)	Protease mutation(s)	IC_{50} (nM) ± SD (change, *n*-fold) of:			
				Zidovudine	Lamivudine	Efavirenz	Lopinavir
JRCSF (B)	R5	None	L63P	1.4 ± 0.6 (1)	13.6 ± 4.6 (1)	0.9 ± 0.1 (1)	19.3 ± 8.4 (1)
1 (B)	R5	None	L63P/T, A71A/V, V77I	1.2 (0.7)	4.2 (0.3)	1.5 (1.8)	6.8 (0.5)
2 (B)	X4, R5	M41L, D67N, K70R, K101Q, M184V, L210L/W, T215F, K219Q	L10I, L33F, M46I, F53L, I54V, L63P, A71V, G73S/T, V77I, V82F, L90M	56.1 (32.9)	>5,000 (>380.7)	1.1 (1.3)	>1,000 (>76.5)
3 (F)	X4, R5	M41L, E44E/D, D67N, K101K/E, V118I, L210W, T215Y	K20T, D30N, M36I, M46M/L, L63P, A71V, N88D	195.1 (114.5)	34.5 (2.6)	0.1 (0.2)	ND[c] (ND)
4 (B)	X4, R5	M41L, E44A, D67N, V118I, L210W, T215Y	L10V, K20T, D30N, M36I, I54V, L63T, A71V, V77V/I, N88D, L90M	326.5 (191.7)	13.5 (1.0)	0.2 (0.2)	123.4 (9.4)
5 (B)	X4, R5	M41L, E44D, D67N, V118I, M184V, L210W, T215Y	L10V, K20R, V32I, M36I, M46L, F53F/L, I54V, L63P, A71V, V82A, L90M	177.4 (104.1)	>5,000 (>380.7)	0.5 (0.6)	986.8 (75.5)
6 (F)	R5	M41L, E44D, D67N, V118I, L210W, T215Y	L10I, K20T, M36I, M46I, F53L, L63L/I/T/P, A71V, I84V, L90M	381.7 (224.0)	88.0 (6.7)	0.3 (0.4)	190.6 (14.6)
7R[a] (B)	X4	K103N	L63C, V77I	2.1 (1.5)	22.3 (1.6)	60.2 (66.8)	7.6 (0.4)

[a] Recombinant HXB2 with patient-derived protease and RT sequences.
[b] The tropism of each virus was determined by using X4-GHOST and R5-GHOST cells.
[c] ND, not determined.

we could easily evaluate culture conditions and their effects on assay results.

These two characteristics confer a great advantage to using the MaRBLE cell lines for screening new antiretroviral agents. They allow both early- and late-phase inhibitor candidates to be evaluated under the same protocol, as the assay permits multiple viral replications. Moreover, monitoring of RL activity allows false-positive results (inhibition by test drugs due to cytotoxicity) to be detected and eliminated. Finally, the use of RL activity greatly improved the efficacy of screening.

The MaRBLE cell lines stably expressed the transfected genes, as confirmed by the stable expression of CD4, CXCR4, and CCR5 on the surfaces of cells maintained in culture for up to 6 months with continuous passage. We also confirmed that the two reporter genes were stably expressed and that IC_{50}s were identical for both newly plated and 6-month-old cultures (data not shown).

In conclusion, we successfully established two unique cell lines, X4-MaRBLE and R5-MaRBLE, which are useful for assaying viral drug resistance and for screening new antiretroviral compounds. Although the cost of phenotypic assays using our cell lines may be less than that of commercial systems, the assays require a biosafety level 3 laboratory, general culture equipment, and a luminometer for readout. Since these are all expensive items, the assay price should be reduced and the assay protocol should be simplified for wider usage of the assay.

ACKNOWLEDGMENTS

We thank Hiroshi Yoshikura, Mari Takizawa, and Mitsuo Honda for their help and discussions. We also thank Claire Baldwin for her help in preparing the manuscript.

This study was supported by a grant from the Human Sciences Foundation and the Program for Promotion of Fundamental Studies in Health Sciences of the National Institute of Biomedical Innovation (NIBIO).

REFERENCES

1. **Ait-Khaled, M., A. Rakik, P. Griffin, A. Cutrell, M. A. Fischl, N. Clumeck, S. B. Greenberg, R. Rubio, B. S. Peters, F. Pulido, J. Gould, G. Pearce, W. Spreen, M. Tisdale, and S. Lafon.** 2002. Mutations in HIV-1 reverse transcriptase during therapy with abacavir, lamivudine and zidovudine in HIV-1-infected adults with no prior antiretroviral therapy. Antivir. Ther. 7:43–51.
2. **Baxter, J. D., D. L. Mayers, D. N. Wentworth, J. D. Neaton, M. L. Hoover, M. A. Winters, S. B. Mannheimer, M. A. Thompson, D. I. Abrams, B. J. Brizz, J. P. Ioannidis, T. C. Merigan, et al.** 2000. A randomized study of antiretroviral management based on plasma genotypic antiretroviral resistance testing in patients failing therapy. AIDS 14:F83–93.
3. **Bento, F. M., D. Takeshita, C. B. Sacramento, T. R. Machado, M. B. Mathor, A. K. Carmona, and S. W. Han.** 2004. Over expression of the selectable marker blasticidin S deaminase gene is toxic to human keratinocytes and murine BALB/MK cells. BMC Biotechnol. 4:29.
4. **Bosch, R. J., G. F. Downey, D. A. Katzenstein, N. Hellmann, L. Bacheler, and M. A. Albrecht.** 2003. Evaluation of cutpoints for phenotypic hypersusceptibility to efavirenz. AIDS 17:2395–2396.
5. **Cingolani, A., A. Antinori, M. G. Rizzo, R. Murri, A. Ammassari, F. Baldini, S. Di Giambenedetto, R. Cauda, and A. De Luca.** 2002. Usefulness of monitoring HIV drug resistance and adherence in individuals failing highly active antiretroviral therapy: a randomized study (ARGENTA). AIDS 16:369–379.
6. **Clevenbergh, P., J. Durant, P. Halfon, P. del Giudice, V. Mondain, N. Montagne, J. M. Schapiro, C. A. Boucher, and P. Dellamonica.** 2000. Persisting long-term benefit of genotype-guided treatment for HIV-infected patients failing HAART. The Viradapt Study: week 48 follow-up. Antivir. Ther. 5:65–70.
7. **Cohen, C. J., S. Hunt, M. Sension, C. Farthing, M. Conant, S. Jacobson, J. Nadler, W. Verbiest, K. Hertogs, M. Ames, A. R. Rinehart, and N. M. Graham.** 2002. A randomized trial assessing the impact of phenotypic resistance testing on antiretroviral therapy. AIDS 16:579–588.
8. **Condra, J. H., W. A. Schleif, O. M. Blahy, L. J. Gabryelski, D. J. Graham, J. C. Quintero, A. Rhodes, H. L. Robbins, E. Roth, M. Shivaprakash, D. Titus, T. Yang, H. Teppler, K. E. Squires, P. J. Deutsch, and E. A. Emini.** 1995. In vivo emergence of HIV-1 variants resistant to multiple protease inhibitors. Nature 374:569–571.
9. **Durant, J., P. Clevenbergh, P. Halfon, P. Delgiudice, S. Porsin, P. Simonet, N. Montagne, C. A. Boucher, J. M. Schapiro, and P. Dellamonica.** 1999. Drug-resistance genotyping in HIV-1 therapy: the VIRADAPT randomised controlled trial. Lancet 353:2195–2199.
10. **Eshleman, S. H., G. Crutcher, O. Petrauskene, K. Kunstman, S. P. Cunningham, C. Trevino, C. Davis, J. Kennedy, J. Fairman, B. Foley, and J. Kop.** 2005. Sensitivity and specificity of the ViroSeq human immunodefi-

ciency virus type 1 (HIV-1) genotyping system for detection of HIV-1 drug resistance mutations by use of an ABI PRISM 3100 genetic analyzer. J. Clin. Microbiol. **43**:813–817.
11. **Fumero, E., and D. Podzamczer.** 2003. New patterns of HIV-1 resistance during HAART. Clin. Microbiol. Infect. **9**:1077–1084.
12. **Gervaix, A., D. West, L. M. Leoni, D. D. Richman, F. Wong-Staal, and J. Corbeil.** 1997. A new reporter cell line to monitor HIV infection and drug susceptibility in vitro. Proc. Natl. Acad. Sci. USA **94**:4653–4658.
13. **Grant, R. M., D. R. Kuritzkes, V. A. Johnson, J. W. Mellors, J. L. Sullivan, R. Swanstrom, R. T. D'Aquila, M. Van Gorder, M. Holodniy, R. M. Lloyd Jr., C. Reid, G. F. Morgan, and D. L. Winslow.** 2003. Accuracy of the TRUGENE HIV-1 genotyping kit. J. Clin. Microbiol. **41**:1586–1593.
14. **Gu, Z., Q. Gao, X. Li, M. A. Parniak, and M. A. Wainberg.** 1992. Novel mutation in the human immunodeficiency virus type 1 reverse transcriptase gene that encodes cross-resistance to 2′,3′- dideoxyinosine and 2′,3′-dideoxycytidine. J. Virol. **66**:7128–7135.
15. **Hachiya, A., S. Aizawa-Matsuoka, M. Tanaka, Y. Takahashi, S. Ida, H. Gatanaga, Y. Hirabayashi, A. Kojima, M. Tatsumi, and S. Oka.** 2001. Rapid and simple phenotypic assay for drug susceptibility of human immunodeficiency virus type 1 using CCR5-expressing HeLa/CD4(+) cell clone 1–10 (MAGIC-5). Antimicrob. Agents Chemother. **45**:495–501.
16. **Hartley, J. W., and W. P. Rowe.** 1976. Naturally occurring murine leukemia viruses in wild mice: characterization of a new "amphotropic" class. J. Virol. **19**:19–25.
17. **Hertogs, K., M. P. de Bethune, V. Miller, T. Ivens, P. Schel, A. Van Cauwenberge, C. Van Den Eynde, V. Van Gerwen, H. Azijn, M. Van Houtte, F. Peeters, S. Staszewski, M. Conant, S. Bloor, S. Kemp, B. Larder, and R. Pauwels.** 1998. A rapid method for simultaneous detection of phenotypic resistance to inhibitors of protease and reverse transcriptase in recombinant human immunodeficiency virus type 1 isolates from patients treated with antiretroviral drugs. Antimicrob. Agents Chemother. **42**:269–276.
18. **Hollinger, F. B., J. W. Bremer, L. E. Myers, J. W. Gold, L. McQuay, and the NIH/NIAID/DAIDS/ACTG Virology Laboratories.** 1992. Standardization of sensitive human immunodeficiency virus coculture procedures and establishment of a multicenter quality assurance program for the AIDS Clinical Trials Group. J. Clin. Microbiol. **30**:1787–1794.
19. **Imamichi, T.** 2004. Action of anti-HIV drugs and resistance: reverse transcriptase inhibitors and protease inhibitors. Curr. Pharm. Des. **10**:4039–4053.
20. **Johnson, V. A., F. Brun-Vezinet, B. Clotet, B. Conway, D. R. Kuritzkes, D. Pillay, J. M. Schapiro, A. Telenti, and D. D. Richman.** 2005. Update of the drug resistance mutations in HIV-1: fall 2005. Top. HIV Med. **13**:125–131.
21. **Kimpton, J., and M. Emerman.** 1992. Detection of replication-competent and pseudotyped human immunodeficiency virus with a sensitive cell line on the basis of activation of an integrated beta-galactosidase gene. J. Virol. **66**:2232–2239.
22. **Larder, B. A., S. D. Kemp, and P. R. Harrigan.** 1995. Potential mechanism for sustained antiretroviral efficacy of AZT-3TC combination therapy. Science **269**:696–699.
23. **Larder, B. A., A. Kohli, P. Kellam, S. D. Kemp, M. Kronick, and R. D. Henfrey.** 1993. Quantitative detection of HIV-1 drug resistance mutations by automated DNA sequencing. Nature **365**:671–673.
24. **Miyake, H., Y. Iizawa, and M. Baba.** 2003. Novel reporter T-cell line highly susceptible to both CCR5- and CXCR4-using human immunodeficiency virus type 1 and its application to drug susceptibility tests. J. Clin. Microbiol. **41**:2515–2521.
25. **Myint, L., M. Matsuda, Z. Matsuda, Y. Yokomaku, T. Chiba, A. Okano, K. Yamada, and W. Sugiura.** 2004. Gag non-cleavage site mutations contribute to full recovery of viral fitness in protease inhibitor-resistant human immunodeficiency virus type 1. Antimicrob. Agents Chemother. **48**:444–452.
26. **Petropoulos, C. J., N. T. Parkin, K. L. Limoli, Y. S. Lie, T. Wrin, W. Huang, H. Tian, D. Smith, G. A. Winslow, D. J. Capon, and J. M. Whitcomb.** 2000. A novel phenotypic drug susceptibility assay for human immunodeficiency virus type 1. Antimicrob. Agents Chemother. **44**:920–928.
27. **Reed, L., and H. Muench.** 1938. A simple method of estimating fifty percent endpoint. Am. J. Hyg. **27**:493–497.
28. **Sarkar, G., and S. S. Sommer.** 1990. The "megaprimer" method of site-directed mutagenesis. BioTechniques **8**:404–407.
29. **Shimizu, Y. K., R. H. Purcell, and H. Yoshikura.** 1993. Correlation between the infectivity of hepatitis C virus in vivo and its infectivity in vitro. Proc. Natl. Acad. Sci. USA **90**:6037–6041.
30. **Shulman, N. S., R. J. Bosch, J. W. Mellors, M. A. Albrecht, and D. A. Katzenstein.** 2004. Genetic correlates of efavirenz hypersusceptibility. AIDS **18**:1781–1785.
31. **Spenlehauer, C., C. A. Gordon, A. Trkola, and J. P. Moore.** 2001. A luciferase-reporter gene-expressing T-cell line facilitates neutralization and drug-sensitivity assays that use either R5 or X4 strains of human immunodeficiency virus type 1. Virology **280**:292–300.
32. **Sugden, B., K. Marsh, and J. Yates.** 1985. A vector that replicates as a plasmid and can be efficiently selected in B-lymphoblasts transformed by Epstein-Barr virus. Mol. Cell. Biol. **5**:410–413.
33. **Tisdale, M., S. D. Kemp, N. R. Parry, and B. A. Larder.** 1993. Rapid in vitro selection of human immunodeficiency virus type 1 resistant to 3′-thiacytidine inhibitors due to a mutation in the YMDD region of reverse transcriptase. Proc. Natl. Acad. Sci. USA **90**:5653–5656.
34. **Tural, C., L. Ruiz, C. Holtzer, J. Schapiro, P. Viciana, J. Gonzalez, P. Domingo, C. Boucher, C. Rey-Joly, and B. Clotet.** 2002. Clinical utility of HIV-1 genotyping and expert advice: the Havana trial. AIDS **16**:209–218.
35. **Vandamme, A. M., F. Houyez, D. Banhegyi, B. Clotet, G. De Schrijver, K. A. De Smet, W. W. Hall, R. Harrigan, N. Hellmann, K. Hertogs, C. Holtzer, B. Larder, D. Pillay, E. Race, J. C. Schmit, R. Schuurman, E. Schulse, A. Sonnerborg, and V. Miller.** 2001. Laboratory guidelines for the practical use of HIV drug resistance tests in patient follow-up. Antivir. Ther. **6**:21–39.
36. **Vodros, D., C. Tscherning-Casper, L. Navea, D. Schols, E. De Clercq, and E. M. Fenyo.** 2001. Quantitative evaluation of HIV-1 coreceptor use in the GHOST3 cell assay. Virology **291**:1–11.
37. **Willey, R. L., R. Shibata, E. O. Freed, M. W. Cho, and M. A. Martin.** 1996. Differential glycosylation, virion incorporation, and sensitivity to neutralizing antibodies of human immunodeficiency virus type 1 envelope produced from infected primary T-lymphocyte and macrophage cultures. J. Virol. **70**:6431–6436.
38. **Wilson, J. W.** 2003. Update on antiretroviral drug resistance testing: combining laboratory technology with patient care. AIDS Read. **13**:25–30, 35–38.
39. **Winters, M. A., R. J. Bosch, M. A. Albrecht, and D. A. Katzenstein.** 2003. Clinical impact of the M184V mutation on switching to didanosine or maintaining lamivudine treatment in nucleoside reverse-transcriptase inhibitor-experienced patients. J. Infect. Dis. **188**:537–540.
40. **Yoshikura, H.** 1989. Thermostability of human immunodeficiency virus (HIV-1) in a liquid matrix is far higher than that of an ecotropic murine leukemia virus. Jpn. J. Cancer Res. **80**:1–5.

THE JOURNAL OF BIOLOGICAL CHEMISTRY VOL. 282, NO. 51, pp. 36923–36932, December 21, 2007

Gp120 V3-dependent Impairment of R5 HIV-1 Infectivity Due to Virion-incorporated CCR5*

Received for publication, June 28, 2007, and in revised form, October 11, 2007 Published, JBC Papers in Press, October 30, 2007, DOI 10.1074/jbc.M705298200

Kazuaki Monde[‡], Yosuke Maeda[‡], Yuetsu Tanaka[§], Shinji Harada[‡], and Keisuke Yusa[‡1]

From the [‡]Department of Medical Virology, Graduate School of Medical Sciences, Kumamoto University, Honjo 1-1-1, Kumamoto 860-8556, Japan and the [§]Department of Infectious Disease and Immunology, Okinawa-Asia Research Center of Medical Science, Faculty of Medicine, University of the Ryukyus, Uehara 207, Nishihara, Okinawa 903-0215, Japan

Entry of R5 human immunodeficiency virus type 1 (HIV-1) into target cells requires sequential interactions of the envelope glycoprotein gp120 with the receptor CD4 and the coreceptor CCR5. We investigated replication of 45 R5 viral clones derived from the HIV-$1_{JR\text{-}FLan}$ library carrying 0–10 random amino acid substitutions in the gp120 V3 loop. It was found that 6.7% (3/45) of the viruses revealed ≥10-fold replication suppression in PM1/CCR5 cells expressing high levels of CCR5 compared with PM1 cells expressing low levels of CCR5. In HIV-$1_{V3L\#08}$, suppression of replication was not associated with entry events and viral production but with a marked decrease in infectivity of nascent progeny virus. HIV-$1_{V3L\#08}$, generated from infected PM1/CCR5 cells, was 98% immunoprecipitated by anti-CCR5 monoclonal antibody T21/8, whereas the other infectious viruses were only partially precipitated, suggesting that incorporation of larger amounts of CCR5 into the virions caused impairment of viral infectivity in HIV-$1_{V3L\#08}$. The results demonstrate the implications of an alternative influence of CCR5 on HIV-1 replication.

Entry of R5 human immunodeficiency virus type 1 (HIV-1)[2] into a target cell requires cooperative interactions of the viral envelope protein gp120 with the receptor CD4 and the coreceptor CCR5 (or CXCR4 for X4 HIV-1) (1–3). These interactions depend on the concentration and distribution of receptor and coreceptor molecules on the cell surface (4–7). Cells with a large amount of CD4 only require trace amounts of CCR5 for maximal susceptibility to infection by R5 HIV-1, whereas cells low in CD4 require larger amounts of CCR5 for maximal infection (6, 8). Sequential binding of the viral surface glycoprotein gp120 to CD4 and CCR5 initiates R5 HIV-1 infection; CD4 attachment induces a conformational change in gp120 that exposes a CCR5 binding domain (9–11). The coreceptor-binding site located in the bridging sheet and the V3 loop of gp120 also play a crucial role in interacting with the N-terminal domains of the CCR5 (12–16). Finally, direct interaction between CCR5 and the V3 loop (35–37 amino acid residues) in gp120 induces structural rearrangements of a fusion peptide of gp41, allowing fusion of viral and cellular membranes (14, 15, 17–19).

Envelope viruses are known to down-modulate the receptor expression on infected cells to prevent reinfection (20, 21). Post-entry, HIV infection leads to a rapid and potent down-modulation of CD4 molecules expressed at the cell surface. Three viral gene products, Nef, Env, and Vpu, are involved in trafficking and catabolism of down-modulating CD4. Nef enhances CD4 internalization and directs the receptor to lysosomes for degradation (22–27), whereas Env and Vpu interfere with the transport of newly synthesized CD4 to the cell surface (28, 29). Without strict CD4 down-modulation, CD4 induces trapping and aggregation of nascent progeny virions at the cell surface by the high affinity of gp120 for CD4 (30) and a dramatic reduction in the infectivity of released virions by recruitment and sequestration of gp120 molecules away from budding sites or recruitment of nonfunctional gp120-CD4 complexes at the virion surface (31, 32).

On the other hand, strict down-modulation of coreceptor CCR5 is not observed in HIV-infected cells, although CCR5 expression on the cell surface is partially reduced by Nef (33). Partial down-regulation of CCR5 and strict down-regulation of CD4 prevent the superinfection of cells in which viral replication is already progressing. CCR5 binding domains, V3 loop, and the bridging sheet domain of gp120 are not exposed until conformational changes in gp120 are induced by interaction with CD4 on the cell surface; therefore, CCR5 would not trap nascent progeny virions at the cell surface. This may be one reason why CCR5 does not need to be strictly down-regulated after viral entry. However, a presence of an unknown inhibitory effect of CCR5 on R5 HIV-1 replication is possible. This paper addresses whether the level of CCR5 in $CD4^+$ T-cell lines influences R5 HIV-1 replication, including late stages of the viral lifecycle. To evaluate the effect of V3 loop on viral replication with respect to CCR5 expression, 45 replication-competent mutant viruses carrying multiple amino acid substitutions in the gp120 V3 loop were used which were derived from an R5 HIV-1 V3 loop library using HIV-$1_{JR\text{-}FLan}$ as background (34). The library contained a set of random combinations of 0–10 polymorphic amino acid substitutions observed in 31 R5 clinical isolates. Replication of the viruses in a $CD4^+$ T-cell line PM1 expressing low levels of CCR5 and PM1/CCR5 cells expressing

* This work was supported by grants from the Ministry of Education, Science, Sports, and Culture and the Ministry of Health Labor and Welfare, Japan, and in part by the Cooperative Research Project on Clinical and Epidemiological Studies of Emerging and Re-emerging Infectious (Renkei Jigyo: no. 78, Kumamoto University). The costs of publication of this article were defrayed in part by the payment of page charges. This article must therefore be hereby marked "*advertisement*" in accordance with 18 U.S.C. Section 1734 solely to indicate this fact.

[1] To whom correspondence should be addressed. Tel.: 81-96-373-5130; Fax: 81-96-373-5132; E-mail: yusak@kumamoto-u.ac.jp.

[2] The abbreviations used are: HIV, human immunodeficiency virus; mAb, monoclonal antibodies; PBS, phosphate-buffered saline; ELISA, enzyme-linked immunosorbent assay.

high levels of CCR5 was examined. It was found that the viruses revealed different replication phenotypes with respect to CCR5 expression. The present study focused on a viral clone, HIV-$1_{V3L\#08}$, with a replication in PM1 cells comparable with wild type HIV-$1_{JR\text{-}FLan}$ but with dramatically suppressed replication in PM1/CCR5 cells. This is the first report that suppression of replication by high expression of CCR5 is V3 loop-dependent and associated with late stages of viral replication.

EXPERIMENTAL PROCEDURES

Cells and Viruses—The human $CD4^+$ T-cell line PM1 (35) was provided by the National Institutes of Health (NIH) AIDS Research and Preference Reagent Program, Division of AIDS NIAID, NIH, and maintained in RPMI1640 (Invitrogen) supplemented with 10% heat-inactivated fetal calf serum (Vitromex). PM1/CCR5 cells were generated by standard retrovirus-mediated transduction of PM1 cells by coculture with PA317 clone #8 cells transfected with pG1TKneo-CCR5 (36) without cloning. MAGIC5 (37) and 293T cells were maintained in Dulbecco's modified Eagle's medium (ICN Biomedicals) supplemented with 10% heat-inactivated fetal calf serum.

pJR-FL_{an} was created in our laboratory from pJR-FL (kindly provided by Dr. Y. Koyanagi, Kyoto University), incorporating AflII and NheI sites into Env at 6395 and 6562 nucleotides, respectively. R5 viruses, carrying a set of random amino acid substitutions in the gp120 V3 loop, were derived from the HIV-1 V3 loop library (34). For construction of V3 loop mutant viruses, amino acid substitutions were introduced into the gp120 V3 loop of pJR-FL_{an}, as described previously (34). For virus preparation, 293T cells (1×10^6) were transfected with 10 μg of molecular clone DNA using the calcium phosphate ProFection Mammalian Transfection System (Promega). The supernatant was collected at 28 h post-transfection and filtered through a 0.22-μm filter unit (Millipore) and stored at −80 °C until use.

HIV-1 single-cycle luciferase reporter viruses were produced by cotransfection of 293T cells with pNL-LucR^-E^- (38) and Env-expressing plasmids pCXN-$Env_{JR\text{-}FLan}$, pCXN-$Env_{JR\text{-}FLan\text{-}A69T}$, pCXN-$Env_{V3L\#08}$, or pCXN-$Env_{V3L\#08\text{-}A69T}$. Culture supernatant containing pseudoviruses at a final concentration of 8 ng/ml p24 was added to 1×10^4 cells/well PM1 or PM1/CCR5 cells in a 48-well plate. After 2 h, the cells were washed twice with phosphate-buffered saline (PBS), and firefly luciferase activity was measured 48 h post-infection according to the manufacturer's directions (Promega).

Viral Replication Assay—For determination of replication phenotype, 4×10^4 of PM1 or PM1/CCR5 cells were infected with 8 ng of p24 Gag for 2 h. After washing twice with PBS, the infected cells were incubated at 37 °C in a 5% CO_2 atmosphere. On day 6 post-infection, p24 Gag in the supernatant was measured using a p24 Gag ELISA (Zeptometrix).

Flow Cytometry—Cell surface expression of CD4 and CCR5 was analyzed by flow cytometry. Cells were incubated in the staining solution (3% fetal calf serum plus 0.05% sodium azide in PBS) with the mouse monoclonal antibodies (mAbs) anti-human CD4 (SK3, BD Biosciences Pharmingen) or anti-human CCR5 (2D7, BD Biosciences Pharmingen) at 4 °C for 30 min. The cells were washed with PBS, and fluorescein isothiocyanate-conjugated goat anti-mouse IgG antibody was used for antibody-staining. Flow cytometry was performed with a FACSCalibur flow cytometer (BD Biosciences) and analyzed with BD Cell Quest Version 3.1 software (BD Biosciences Pharmingen).

Quantitative PCR—Virus (8 ng p24 Gag) was pretreated in culture fluids with 690 units of DNase I (Worthington Biochem) and added to PM1 or PM1/CCR5 cells (4×10^4) for 2 h at 37 °C. Cells were then washed and incubated at 37 °C for 8 h. Total DNA was purified using the QIAamp DNA blood kit (Qiagen) and eluted in a total volume of 200 μl. Two μl of DNA was analyzed by real-time quantitative PCR. Late reverse transcription products were detected using primers amplifying the region between nucleotides 685 and 789 of the provirus: forward primer (5′-ACATCAAGCAGCCATGCAAAT-3′), reverse primer (5′-ATCTGGCCTGGTGCAATAGG-3′), and probe (5′-FAM-CATCAATGAGGAAGCTGCAGAATGG-GATAGA-TAMRA-3′). Reactions were performed in triplicate in TaqMan Universal PCR master mix using 0.9 pmol of each primer/μl and 0.25 pmol of probe/μl. After 10 min at 95 °C, reactions were cycled for 15 s at 95 °C followed by 1 min at 60 °C for 40 repeats on an ABI Prism model 7700 thermal cycler (Applied Biosystems).

Virus Infectivity Assay—For infectivity assay, 5×10^3 of MAGIC5 cells (37) were plated 1 day before infection into 48-well tissue culture plates. After absorption of virus for 2 h at 37 °C, cells were washed twice with PBS and further incubated at 37 °C in 5% CO_2. At 48 h post-infection, the cells were stained, and the number of blue foci in each well was counted (39).

Western Blot Analysis—Four days post-infection, viruses in the supernatant of HIV-1-infected cells were pelleted by centrifugation at 175,000 × *g* for 60 min. Viral proteins (10 ng of p24 Gag) were separated by 4–20% SDS-PAGE, transferred to a polyvinylidene difluoride Immobilon P membrane (Millipore), and blocked with 5% milk in PBST (137 mM NaCl, 8.1 mM Na_2HPO_4, 2.68 mM KCl, 1.47 mM KH_2PO_4, and 0.05% Tween 20) for 8 h at room temperature. Immunodetection was performed with anti-gp120 antibody (Aalto Bio Reagents) and anti-gp41 antibody (2F5; National Institutes of Health AIDS Research and Preference Regent Program) followed by a secondary antibody conjugated to horseradish peroxidase (Sigma) and Chemi-Lumi One (Nacalai Tesque).

Virus Precipitation Assay—Virus immunoprecipitation assay was performed as described previously (40). Anti-HLA-DR (L243), anti-CCR5 (3A9), and anti-CXCR4 (12G5) mAbs were purchased from BD Biosciences Pharmingen. Anti-CCR5 (T21/8) mAb was purchased from BioLegend. A rat immunoglobulin G1 (IgG1) mAb against hepatitis C virus, Mo-8 (41), was used as a rat isotype-matched negative control. Virus (5 ng of p24 Gag) in PBS containing 3% bovine serum albumin was mixed with the mAb at a concentration of 10 μg/ml in a final volume of 100 μl and incubated for 12 h at 4 °C. Then, 10 μl of Pansorbin (Calbiochem), a suspension of heat-killed *Staphylococcus aureus* cells pretreated for 1 h with 3% bovine serum albumin, was added to the virus/mAb mixture. After incubation for 30 min at room temperature, captured viruses were

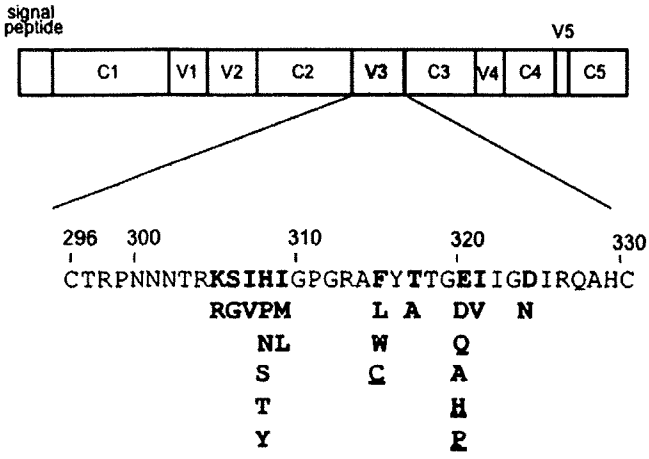

FIGURE 1. **Amino acid substitutions of the R5 HIV-1 V3 loop library.** Each viral clone contained 0–10 substitutions in the gp120 V3 loop. pJR-FL_{an} was used to construct the library as background. Theoretically, the number of possible combinations of 0–10 amino acid substitutions was calculated as 27,648. Residues in *boldface* indicate the substitutions that were randomly incorporated. *Underlined* residues indicate the substitutions that were not detected in the 31 R5 viruses, Phe^{315} to Cys or Glu^{320} to His or Pro but inevitably incorporated into the library due to combinations of nucleotide substitutions.

removed by centrifugation (350 × *g* for 30 min). p24 Gag in the supernatant was determined by p24 Gag ELISA.

RESULTS

Replication Suppression of Viruses from the R5 HIV-1 V3 Loop Library in PM1/CCR5 Cells—An R5 HIV-1 V3 loop library was constructed carrying a set of random combinations of 0–10 amino acid substitutions in the V3 loop (34) (Fig. 1). Replication of 45 viruses randomly selected from the library was compared in PM1 and PM1/CCR5 cells (Table 1). PM1/CCR5 cells, generated by standard retrovirus transduction of PM1 cells with a CCR5 expression lentivector, regularly expressed high level of CCR5 and with similar levels of CD4 compared with PM1 cells (Fig. 2). A total of 36% of the viruses (16/45) failed to replicate in both cell types (<1.0 ng/ml p24 Gag on day 6). Among replication competent viruses, ratios of p24 Gag ranged from ≤0.1 to 27, whereas the parental virus, HIV-$1_{JR\text{-}FLan}$, could replicate in both PM1 and PM1/CCR5 cells (ratio 1.9). Viruses were classified into the following three groups; 1) those that grew ≥10-fold more in PM1/CCR5 than PM1 cells (ratio ≥ 10), designated $R5^H$ phenotype, 2) those that revealed comparative replication kinetics in PM1 and PM1/CCR5 cells (0.1 < ratio < 10), designated $R5^{HL}$, and 3) viruses where replication was drastically suppressed in PM1/CCR5 cells (ratio ≤ 0.1), designated $R5^L$. Six of 45 viruses (13%), including HIV-$1_{V3L\#10}$, HIV-$1_{V3L\#16}$, HIV-$1_{V3L\#21}$, HIV-$1_{V3L\#23}$, HIV-$1_{V3L\#29}$, and HIV-$1_{V3L\#34}$, were classified as $R5^H$ phenotype, whereas 3 of the 45 (6.7%) viral clones, HIV-$1_{V3L\#08}$, HIV-$1_{V3L\#23}$, and HIV-$1_{V3L\#25}$, were $R5^L$ phenotype. These results indicated that the R5 HIV-1 V3 loop library contained unique replication phenotypes with respect to expression levels of CCR5 in the $CD4^+$ T-cell line. Note that these viruses carried amino acid substitutions in the V3 loop alone, indicating that the variety of replication phenotypes was dependent on their V3 loop structure.

Attention was then focused on the $R5^L$ phenotype, HIV-$1_{V3L\#08}$, to ascertain why high expression of CCR5 had a suppressive effect on viral replication. Replication of HIV-$1_{V3L\#08}$ was markedly suppressed in PM1/CCR5 cells, whereas the virus showed similar replication kinetics to HIV-$1_{JR\text{-}FLan}$ with 8 ng of p24 Gag in PM1 cells (Fig. 3, *A* and *B*). On day 6 post-infection, p24 Gag in the supernatant was 33-fold lower in PM1/CCR5 than PM1 cells. However, no replication suppression of HIV-$1_{V3L\#08}$ was observed in peripheral blood mononuclear cells or macrophages derived from three different donors compared with HIV-$1_{JR\text{-}FLan}$ (data not shown). HIV-$1_{V3L\#08}$ contained 8 amino acid substitutions: Ile^{307} to Val, His^{308} to Thr, Ile^{309} to Met, Phe^{315} to Leu, Thr^{317} to Ala, Glu^{320} to Asp, Ile^{321} to Val, and Asp^{324} to Asn in gp120 V3 loop alone (Fig. 3*C*).

A revertant of HIV-$1_{V3L\#08}$, designated HIV-$1_{V3L\#08\text{-}A69T}$, was isolated that restored replication ability in PM1/CCR5 cells with an additional substitution Ala^{69} to Thr in the C1 region of gp120 (Fig. 3*C*). HIV-$1_{JR\text{-}FLan\text{-}A69T}$ and HIV-$1_{V3L\#08\text{-}A69T}$ showed similar replication kinetics to HIV-$1_{JR\text{-}FLan}$ in PM1 cells (Fig. 3*A*). However, HIV-$1_{JR\text{-}FLan\text{-}A69T}$ and HIV-$1_{V3L\#08\text{-}A69T}$ showed a slightly higher replication profile in PM1/CCR5 cells on days 4 and 5 compared with HIV-$1_{JR\text{-}FLan}$ (Fig. 3*B*).

It is possible that suppression of HIV-$1_{V3L\#08}$ replication in PM1/CCR5 cells was due to high susceptibility of the virus to the chemokine(s) produced by the cells. To exclude this possibility, susceptibility of HIV-$1_{V3L\#08}$, HIV-$1_{V3L\#08\text{-}A69T}$, HIV-$1_{JR\text{-}FLan}$, and HIV-$1_{JR\text{-}FLan\text{-}A69T}$ to a β-chemokine, RANTES (regulated on activation normal T cell expressed and secreted), was measured, but no differences were detected (data not shown).

Entry Efficiency of HIV-$1_{V3L\#08}$ into PM1/CCR5 Cells—To investigate whether the entry efficiency of HIV-$1_{V3L\#08}$ decreased, real-time PCR was utilized to analyze cellular accumulation of the late reverse transcriptase product, *gag*, synthesized shortly after virus entry into the cells (Fig. 4*A*). There was no decrease in *gag* DNA synthesis of HIV-$1_{V3L\#08}$ in PM1/CCR5 compared with PM1 cells. Rather, the DNA copies of HIV-$1_{V3L\#08}$ were 3.3-fold higher in PM1/CCR5 than in PM1 cells. Higher expression of CCR5 could promote more efficient viral entry when CD4 is not significantly expressed, consistent with previous reports for other viruses (1.9–2.5-fold) (6, 8). Moreover, there was no clear difference in DNA synthesis among the four viruses in PM1/CCR5 cells.

In addition, the virus pseudotyped with the envelope proteins of HIV-$1_{V3L\#08}$ revealed 2.0-fold more efficiency in PM1/CCR5 than in PM1 cells (Fig. 4*B*). Luciferase activity of other viruses in PM1/CCR5 cells also increased 1.7–2.2-fold compared with PM1 cells. Measured luciferase activity in cells infected with pseudotyped viruses serves as an indirect estimation of viral entry, integration, and transcriptional activity. The results demonstrate that suppression of HIV-$1_{V3L\#08}$ replication in PM1/CCR5 cells is not associated with early stages of the viral lifecycle.

Production of Virus from PM1/CCR5 Cells Infected with HIV-$1_{V3L\#08}$—A comparison was made of the number of virions generated from PM1/CCR5 and PM1 cells in the presence of a reverse transcriptase inhibitor (AZT) and a CCR5 inhibitor

TABLE 1
Replication of viruses from the HIV-1 V3 loop library in PM1 and PM1/CCR5 cells

Viral clone	V3 sequence	p24 Gag antigen (ng/ml)[a]		
		PM1	PM1/CCR5	Ratio[b]
$HIV\text{-}1_{JR\text{-}FLan}$	CTRPNNNTRKSIHIGPGRAFYTTGEIIGDIRQAHC	140	270	1.9
#01	.....RG.PM.....HV.....	18	50	2.8
#02	.....L.....L.A..D...N.....	17	54	3.2
#03	.....RG.PL.....C.A..AV.....	<1.0	<1.0	–
#04	.....RGVYL.....PV.....	<1.0	<1.0	–
#05	.....R..NL.....L.....V..N.....	70	49	0.7
#06	.....R.VS.....L.A...V..N.....	46	17	0.4
#07	.....RG.PM.....W.A..H.....	23	20	0.9
#08	.....VTM.....L.A..DV..N.....	83	8.0	0.1
#09	.....GVNL.....L.A..DV.....	51	20	0.4
#10	.....S.....A..HV..N.....	21	220	10
#11	.....RGV.L.....PV.....	<1.0	<1.0	–
#12	.....VN.....A..PI..N.....	<1.0	<1.0	–
#13	.....R.VNL.....W....Q.....	4.0	5.0	1.3
#14	.....RGVPL.....A.....	<1.0	<1.0	–
#15	.....G..L.....C....H...N.....	<1.0	<1.0	–
#16	.....RG.YM.....L....QV.....	6.0	160	27
#17	.....RGVPL.....A..DV..N.....	3.0	10	3.3
#18	.....YL.....L....P...N.....	<1.0	<1.0	–
#19	.....GVT.....W.A.....	38	29	0.8
#20	.....RGVYM.....C....A...N.....	<1.0	<1.0	–
#21	.....NL.....Q...N.....	7.0	140	20
#22	.....VPM.....A.VAV..N.....	5.0	53	11
#23	.....VNM.....L....D.....	120	14	0.1
#24	.....R.VPL.....W.A.....N.....	3.0	3.0	1.0
#25	.....R.V.M.....V..N.....	70	6.0	0.1
#26	.....GVTL.....L.....V.....	<1.0	<1.0	–
#27	.....GVNL.....L.....V.....	13	8.0	0.6
#28	.....G.PL.....L.A..HV..N.....	40	47	1.2
#29	.....RG.PM.....PV..N.....	7.0	100	27
#30	.....SM.....W.A..P...N.....	2.0	2.0	1.0
#31	.....L.....C....H...N.....	<1.0	<1.0	–
#32	.....RG..L.....L.....N.....	3.0	3.0	1.0
#33	.....T.....W....PV..N.....	3.0	5.0	1.7
#34	.....GVYM.....L.S..D.....	7.0	170	24
#35	.....RGV.L.....W.A..H...N.....	2.0	2.0	1.0
#36	.....RG.....H.....	3.0	3.0	1.0
#37	.....TM.....L.A..P...N.....	<1.0	<1.0	–
#38	.....G.Y.....D.....	3.0	23	7.7
#39	.....Y.....P.....	5.0	37	7.4
#40	.....RG.TL.....W.A.....	<1.0	<1.0	–
#41	.....G..M.....C....PV..N.....	<1.0	<1.0	–
#42	.....RG.....L.A..PV..N.....	<1.0	<1.0	–
#43	.....L.....L.A..PV.....	60	24	0.4
#44	.....VP.....C.A..A...N.....	<1.0	<1.0	–
#45	.....RGET.....L....AV..N.....	<1.0	<1.0	–

[a] PM1 or PM1/CCR5 cells (4×10^4) were infected with each virus (8 ng of p24 Gag). On day 6 the extent of viral replication was measured by p24 Gag ELISA. Results represent the average of three independent experiments.
[b] Ratio, the concentration of p24 Gag in the supernatant of PM1/CCR5 cells was divided by that of PM1 cells.

(TAK-779) to block secondary infection by nascent progeny virus. The concentrations of AZT and TAK-779 used were 4 and 1 μM, respectively, 78- and 32-fold higher than the respective IC_{50} levels (the concentration required to inhibit 50% of the blue foci formation in MAGIC5 cells) (data not shown). Note that on day 2 post-infection, the number of viruses generated from

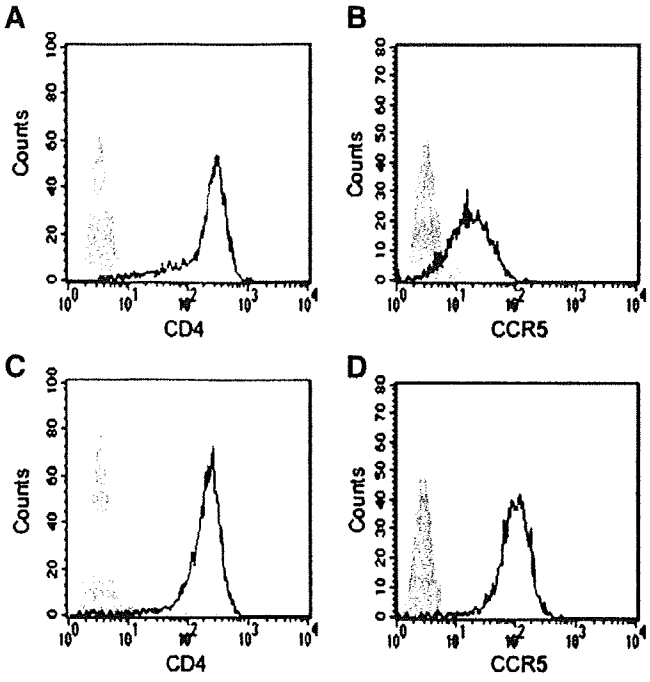

FIGURE 2. **Expression of CD4 and CCR5 in PM1 and PM1/CCR5 cells.** The cells were stained with mAb directed against CD4 (SK3) or CCR5 (2D7) and analyzed by flow cytometry. *A*, CD4 in PM1 cells. *B*, CCR5 in PM1 cells. *C*, CD4 in PM1/CCR5 cells; *D*, CCR5 in PM1/CCR5 cells. The *shaded histograms* indicate background staining with secondary antibody alone. The *open histograms* represent staining with indicated primary antibody.

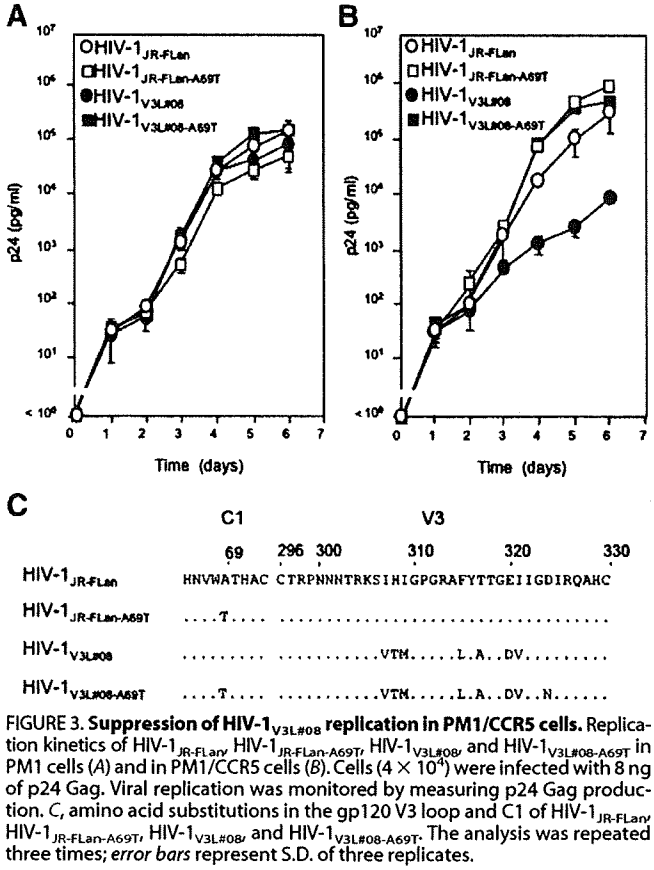

FIGURE 3. **Suppression of HIV-$1_{V3L\#08}$ replication in PM1/CCR5 cells.** Replication kinetics of HIV-$1_{JR\text{-}FLan}$, HIV-$1_{JR\text{-}FLan\text{-}A69T}$, HIV-$1_{V3L\#08}$, and HIV-$1_{V3L\#08\text{-}A69T}$ in PM1 cells (*A*) and in PM1/CCR5 cells (*B*). Cells (4×10^4) were infected with 8 ng of p24 Gag. Viral replication was monitored by measuring p24 Gag production. *C*, amino acid substitutions in the gp120 V3 loop and C1 of HIV-$1_{JR\text{-}FLan}$, HIV-$1_{JR\text{-}FLan\text{-}A69T}$, HIV-$1_{V3L\#08}$, and HIV-$1_{V3L\#08\text{-}A69T}$. The analysis was repeated three times; *error bars* represent S.D. of three replicates.

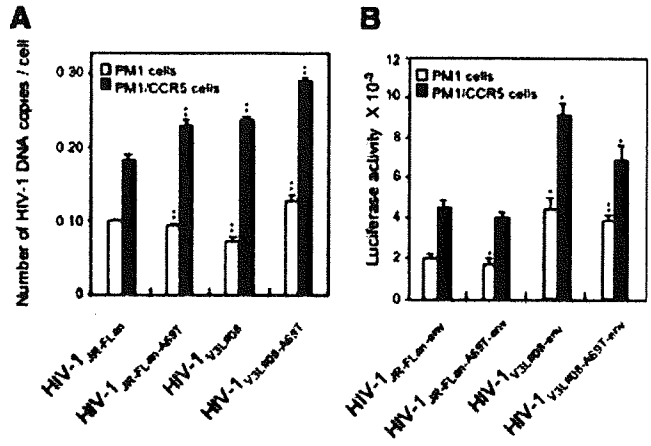

FIGURE 4. **Entry of HIV-$1_{JR\text{-}FLan}$, HIV-$1_{JR\text{-}FLan\text{-}A69T}$, HIV-$1_{V3L\#08}$, and HIV-$1_{V3L\#08\text{-}A69T}$ into PM1 or PM1/CCR5 cells.** *A*, PM1 and PM1/CCR5 cells were infected with 30 ng of p24 HIV-1 for 2 h. Eight hours after infection, synthesized proviral HIV-1 DNA was determined by *Taq*Man real-time PCR. *B*, PM1 or PM1/CCR5 cells were infected for 2 h with viruses pseudotyped with the envelope of HIV-$1_{JR\text{-}FLan}$, HIV-$1_{JR\text{-}FLan\text{-}A69T}$, HIV-$1_{V3L\#08}$, or HIV-$1_{V3L\#08\text{-}A69T}$ (8 ng of p24 Gag). At 48 h post-infection, luciferase activity in cell lysate was determined. The analysis was repeated three times; *error bars* represent the S.D. of three replicates. *, $p < 0.01$; **, $p < 0.001$. Statistical significant differences were calculated by *t* test *versus* HIV-$1_{JR\text{-}FLan}$.

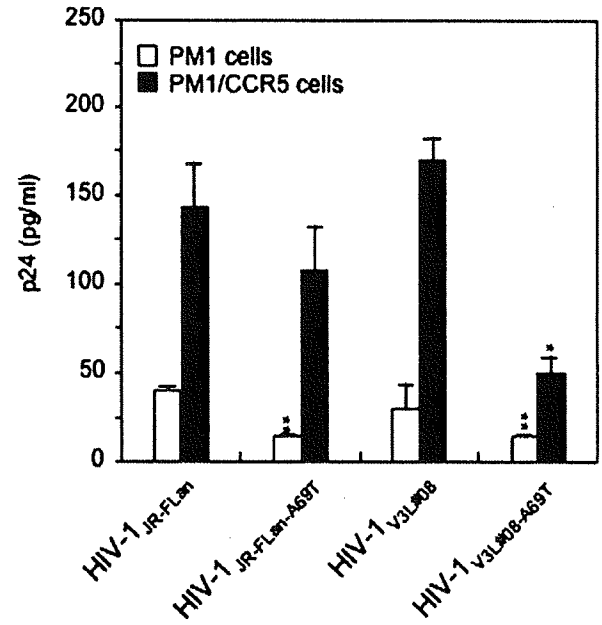

FIGURE 5. **Production of HIV-$1_{JR\text{-}FLan}$, HIV-$1_{JR\text{-}FLan\text{-}A69T}$, HIV-$1_{V3L\#08}$, and HIV-$1_{V3L\#08\text{-}A69T}$ from PM1 or PM1/CCR5 cells in the presence of AZT and TAK-779.** The cells were infected with each virus (8 ng of p24 Gag) for 2 h, then 1 μM AZT and 4 μM TAK779 were added. On day 2, the level of p24 Gag in the supernatant was determined by p24 Gag ELISA. The analysis was repeated three times; *error bars* represent the S.D. of three replicates. *, $p < 0.01$; **, $p < 0.001$. Statistical significant differences were calculated by *t* test *versus* HIV-$1_{JR\text{-}FLan}$.

HIV-$1_{V3L\#08}$-infected PM1/CCR5 cells was 5.7-fold higher than PM1-infected cells (Fig. 5). HIV-$1_{JR\text{-}FLan}$, HIV-$1_{JR\text{-}FLan\text{-}A69T}$, HIV-$1_{V3L\#08}$, and HIV-$1_{V3L\#08\text{-}A69T}$ showed similar results. Production of these viruses generated from PM1/CCR5 cells was 3.8–8.7-fold higher than from PM1 cells, demonstrating that V3 loop structure of HIV-$1_{V3L\#08}$ did not affect viral assembly and budding. Increased virus production from PM1/CCR5 cells was

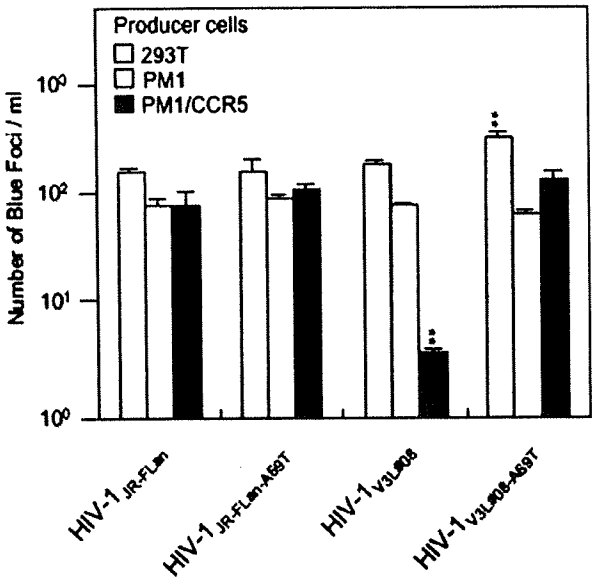

FIGURE 6. **Viral infectivity of HIV-$1_{JR-FLan}$, HIV-$1_{JR-FLan-A69T}$, HIV-$1_{V3L\#08}$, and HIV-$1_{V3L\#08-A69T}$ generated from 293T, PM1, or PM1/CCR5 cells.** Viral infectivity was determined with MAGIC5 cells (HeLa cells expressing CD4 and CCR5 and containing β-galactosidase expression cassettes driven by the HIV-1 long terminal repeat). MAGIC5 cells were infected with each virus for 2 h. At 48 h post-infection, the cells were fixed and stained with 5-bromo-4-chloro-3-indolyl-β-D-galactoside. The number of blue foci was counted in triplicate. The analysis was repeated three times; *error bars* represent S.D. of three replicates. *, $p < 0.01$; **, $p < 0.001$. Statistical significant differences were calculated by *t* test *versus* HIV-$1_{JR-FLan}$.

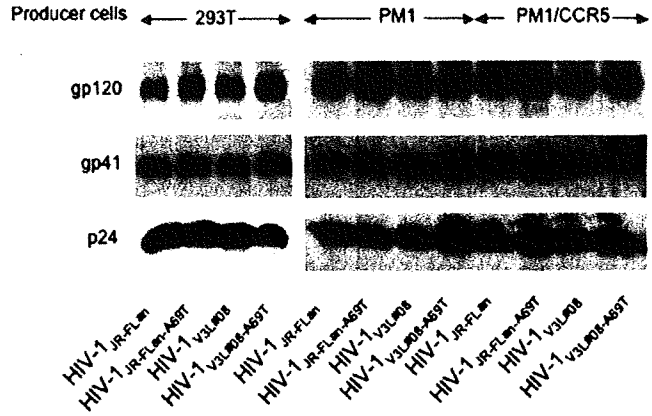

FIGURE 7. **Incorporation of gp120 and gp41 into virus.** HIV-$1_{JR-FLan}$, HIV-$1_{JR-FLan-A69T}$, HIV-$1_{V3L\#08}$, and HIV-$1_{V3L\#08-A69T}$ (100 ng of p24 Gag) produced from 293T, PM1, or PM1/CCR5 cells was resolved by 4–20% SDS-PAGE. Western blot analysis was performed using polyclonal antibody to gp120, gp41, and p24 Gag.

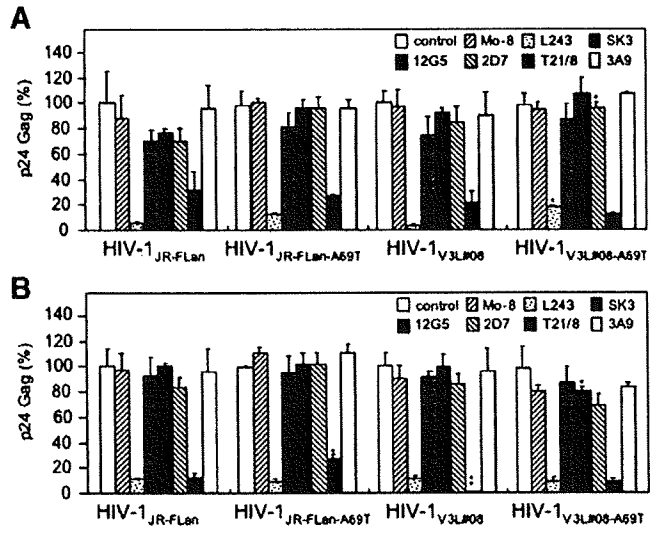

FIGURE 8. **Incorporation of CCR5 into virus.** Virus immunoprecipitation assay was performed using mAbs directed against hepatitis C virus (MO-8), HLA-DR (L243), CD4 (SK3), CXCR4 (12G5), or CCR5 (2D7, T21/8, 3A9). Cell-free virus (5 ng), produced from PM1 (*A*) or PM1/CCR5 (*B*) cells was incubated with 1 μg of mAb for 8 h. Virus-antibody complex were precipitated by the addition of Pansorbin cells. After precipitation of the virus-antibody complex, p24 Gag in supernatants were determined by p24 Gag ELISA. The analysis was repeated three times; *error bars* represent S.D. of three replicates. *, $p < 0.01$; **, $p < 0.001$. Statistical significant differences were calculated by *t* test *versus* HIV-$1_{JR-FLan}$.

consistent with the higher entry efficiency, as shown in Fig. 4, although the increased levels were not equal. This excluded the possibility that replication suppression of HIV-$1_{V3L\#08}$ in PM1/CCR5 cells was due to decreased virus production.

HIV-$1_{V3L\#08}$ Infectivity Generated from PM1/CCR5 Cells—To further investigate replication suppression of HIV-$1_{V3L\#08}$ in PM1/CCR5 cells, infectivity of viruses generated from 293T, PM1, and PM1/CCR5 cells was determined using MAGIC5 cells containing a β-galactosidase gene driven by the HIV long terminal repeat (37) (Fig. 6). Infectivity from 293T cells, used for experimental preparation of viruses, was similar among the four viruses. However, infectivity of HIV-$1_{V3L\#08}$ generated from PM1/CCR5 cells showed a 20-fold decrease compared with HIV-$1_{JR-FLan}$, whereas infectivity of viruses, including HIV-$1_{V3L\#08}$ from PM1 cells, revealed similar infectivity. Note that HIV-$1_{V3L\#08-A69T}$, with an additional substitution of Ala^{69} to Thr plus the eight amino acid substitutions of HIV-$1_{V3L\#08}$, reacquired a potent infection ability from PM1/CCR5 cells. The decrease infectivity in progeny HIV-$1_{V3L\#08}$ from PM1/CCR5 cells could result in impaired replication of HIV-$1_{V3L\#08}$ in PM1/CCR5 cells, as shown in Fig. 3*B*.

CCR5 Incorporation into HIV-$1_{V3L\#08}$ Virions—To elucidate the significance of CCR5 levels on decreased infectivity in HIV-$1_{V3L\#08}$, we examined whether high expression of CCR5 inhibits its incorporation of Env proteins gp120 and gp41 into virus particles. Amounts of gp120 and gp41 on the virus envelopes were compared (Fig. 7). There was no decrease in gp120 and gp41 in HIV-$1_{V3L\#08}$ generated from PM1/CCR5 cells, indicating that high levels of CCR5 has no effect on the incorporation efficiency of gp120 and gp41 into the virions. A slight increase in gp120 and gp41 incorporation into virions was observed in HIV-$1_{JR-FLan-A69T}$ and HIV-$1_{V3L\#08-A69T}$ compared to HIV-$1_{JR-FLan}$ and HIV-$1_{V3L\#08}$ generated from 293T, PM1, and PM1/CCR5 cells. The increased gp120 and gp41 incorporation into virions by the addition of A69T may be in compensation for the loss of infectivity in HIV-$1_{V3L\#08}$ from PM1/CCR5 cells.

Another putative mechanism could be that CCR5 is incorporated into virus particles and specifically impaired the intrinsic function of HIV-$1_{V3L\#08}$ gp120. To examine this possibility, the virions were precipitated using anti-CCR5 mAbs (Fig. 8, *A* and *B*). It has been reported that HLA-DR is incorporated into the viral envelope from the infected cell membrane (42, 43). We confirmed that an anti-HLA-DR mAb L243 could precipitate

TABLE 2
Replication of HIV-1 containing one amino acid substitution in V3 loop in PM1 and PM1/CCR5 cells

Viral clone	V3 loop sequence	p24 Gag (ng/ml)[a] PM1	PM1/CCR5	Ratio[b]
HIV-$1_{JR-Flan}$	CTRPNNNTRKSIHIGPGRAFYTTGEIIGDIRQAHC	140	270	1.9
HIV-$1_{V3\#08}$	.....VTM.....L.A..DV..N.....	83	8.0	0.1
HIV-1_{I307V}	.....V.....	100	11	0.1
HIV-1_{H308T}	.....T.....	79	100	1.3
HIV-1_{I309M}	.....M.....	63	9.0	0.1
HIV-1_{F315L}	.....L.....	59	14	0.2
HIV-1_{T317A}	.....A.....	<1.0	<1.0	–
HIV-1_{E320D}	.....D.....	110	72	0.7
HIV-1_{I321V}	.....V.....	91	110	1.2
HIV-1_{D324N}	.....N.....	75	68	0.9

[a] PM1 or PM1/CCR5 cells (4×10^4) were infected with each virus (8 ng of p24 Gag). On day 6 the extent of viral replication was measured by p24 Gag ELISA. Results represent the average of three independent experiments.
[b] Ratio, the concentration of p24 Gag in the supernatant of PM1/CCR5 cells was divided by that of PM1 cells.

virions generated from PM1 or PM1/CCR5 cells, whereas anti-E2 protein mAb of hepatitis C virus Mo-8, anti-CD4 mAb SK3, or anti-CXCR4 12G5 could not. mAb 2D7 (44), which could recognize the second extracellular loop of CCR5 on the surface of PM1 or PM1/CCR5 cells via flow cytometry (Fig. 2), failed to precipitate viral particles (Fig. 8, *A* and *B*). Similarly, 3A9 (45), an anti-CCR5 mAb recognizing the N terminus via flow cytometry (data not shown), could not precipitate viruses either. Surprisingly, another anti-CCR5 mAb (T21/8), also recognizing the N terminus, partially precipitated viruses generated from PM1 (Fig. 8*A*) and PM1/CCR5 cells (Fig. 8*B*) but not from 293T cells (data not shown). Note that HIV-$1_{V3L\#08}$ generated from PM1/CCR5 cells was almost completely precipitated (98%) by mAb T21/8 (Fig. 8*B*), whereas HIV-$1_{V3L\#08}$ generated from PM1 cells and the other three viruses from both cell types were partially precipitated (69 – 88%) by mAb T21/8 (Fig. 8*A*). The results indicate that sufficient levels of CCR5 were incorporated into HIV-$1_{V3L\#08}$ particles to be precipitated by T21/8. The larger amount of incorporated CCR5 reduced viral infectivity in HIV-$1_{V3L\#08}$, although the recruitment of CCR5 into virions and the molecular mechanism of decreased infectivity in HIV-$1_{V3L\#08}$ are unclear. For comparison of the amount of CCR5 at the surface of the virions, we purified virions by precipitation using anti-gp120 antibody 2G12 from exosomes contaminated in the virion by Western blot analysis. However, we could not detect CCR5 possibly because of low affinity of anti-CCR5 antibodies (data not shown).

Amino Acid Substitutions in the V3 Loop Responsible for $R5^L$ Phenotype—In 45 viral clones, three viruses revealed an $R5^L$ phenotype (Table 1). The amino acid substitutions Ile^{307} to Val and Ile^{309} to Met were common to all three viruses, suggesting that these two substitutions could be responsible for the $R5^L$ phenotype. To assess the contribution of the eight substitutions in the HIV-$1_{V3L\#08}$ V3 loop to the $R5^L$ phenotype, eight V3 loop mutant viruses containing one substitution each were prepared, and their replication phenotypes were determined (Table 2). Replication of HIV-1_{I307V} and HIV-1_{I309M} was suppressed in PM1/CCR5 cells, whereas these viruses could replicate in PM1 cells (>60 ng/ml p24 Gag), consistent with the common substitutions obtained in three $R5^L$ viruses described above (Table 1).

To ascertain the importance of these substitutions, V3 mutant viruses containing random combinations of between two and six of the eight substitutions from HIV-$1_{V3L\#08}$ were prepared. Most of the recombinant viruses preferentially replicate in PM1 cells (ratio $\leq$ 0.5) (Table 3). Four of 12 viruses revealed a $R5^L$ phenotype (ratio $\leq$ 0.1) and contained I307V and/or I309M. Viruses containing I307V always showed a low p24 Gag ratio (ratio $\leq$ 0.3), whereas ratios in I309M-containing viruses were not as low (Fig. 9), *e.g.* 1.4 for HIV-$1_{V3L\#130}$ (Table 3). In addition, F315L frequently conferred a low p24 Gag ratio combined with other substitutions, although F315L alone could not confer $R5^L$ phenotype. The results show that the $R5^L$ phenotype cannot be conferred by just one or two substitutions; a combination of several substitutions, including key substitutions, is essential. The key amino acid residues at 307 and 309 were directly at the N-terminal of the GPGR sequence in the V3 loop crown, suggesting that the amino acid substitutions adjoining the V3 crown may be important in regulating replication kinetics in cells expressing high levels of CCR5.

DISCUSSION

We investigated the replication ability of 45 viral clones from the R5 HIV-1 V3 loop library and found that the library contained different replication phenotypes with respect to the expression level of CCR5 (Table 1). The report focused on one of the viruses, HIV-$1_{V3L\#08}$, that was suppressed 33-fold in PM1/CCR5 cells expressing high levels of CCR5 compared with parental PM1 cells (Fig. 3*B*). This suppression of viral growth was not associated with early events in the lifecycle but with a decrease in viral infectivity in nascent progeny virus from cells expressing high levels of CCR5. MAGIC5 (37) and NP2/CD4/hiCCR5 cells expressed CD4 at levels similar to and CCR5 at levels compatible to or higher than that of PM1/CCR5 cells;